mathematics

MDPI

Article

A Hybrid TLBO-Cheetah Algorithm for Multi-Objective Optimization of SOP-Integrated Distribution Networks

Abdulaziz Alanazi [1,*], Mohana Alanazi [2] and Mohammed Alruwaili [1]

[1] Department of Electrical Engineering, College of Engineering, Northern Border University, Ar'Ar 73222, Saudi Arabia; mohammed.alruwailir@nbu.edu.sa
[2] Department of Electrical Engineering, College of Engineering, Jouf University, Sakaka 72388, Saudi Arabia; msanazi@ju.edu.sa
* Correspondence: af.alanazi@nbu.edu.sa

Abstract

The integration of Soft Open Points (SOPs) into distribution networks has been an essential method for enhancing operational flexibility and efficiency. But simultaneous optimization of network reconfiguration and SOP scheduling constitutes a difficult mixed-integer nonlinear programming (MINLP) problem that is likely to suffer from premature convergence with standard metaheuristic solvers, particularly in large power networks. This paper proposes a novel hybrid algorithm, hTLBO–CO, which synergistically integrates the exploitative capability of Teaching–Learning-Based Optimization (TLBO) with the explorative capability of the Cheetah Optimizer (CO). One of the notable contributions of our framework is an in-depth problem formulation that enables SOP locations on both tie and sectionalizing switches with an efficient constraint-handling scheme, preserving topo-logical feasibility through a minimum spanning tree repair scheme. The evolved hTLBO–CO algorithm is systematically validated across IEEE 33-, 69-, and 119-bus test feeders with differential operational scenarios. Results indicate consistent dominance over established metaheuristics (TLBO, CO, PSO, JAYA), showing significant efficiency improvement in power loss minimization, voltage profile enhancement, and convergence rate. Remarkably, in a situation with a large-scale 119-bus power grid, hTLBO–CO registered a significant 50.30% loss reduction in the single-objective reconfiguration-only scheme, beating existing state-of-the-art approaches by over 15 percentage points. These findings, further substantiated by comprehensive statistical and multi-objective analyses, confirm the proposed framework's superiority, robustness, and scalability, establishing hTLBO–CO as a robust computational tool for the advanced optimization of future distribution networks.

Keywords: hybrid evolutionary algorithms; multi-objective optimization; large-scale optimization; distribution network reconfiguration; soft open points; constraint-handling techniques

MSC: 90B05

check for updates

Academic Editor: Mariona Vila Bonilla

Received: 6 October 2025
Revised: 19 October 2025
Accepted: 22 October 2025
Published: 27 October 2025

Citation: Alanazi, A.; Alanazi, M.; Alruwaili, M. A Hybrid TLBO-Cheetah Algorithm for Multi-Objective Optimization of SOP-Integrated Distribution Networks. *Mathematics* **2025**, *13*, 3419. https://doi.org/10.3390/math13213419

Copyright: © 2025 by the authors. Licensee MDPI, Basel, Switzerland. This article is an open access article distributed under the terms and conditions of the Creative Commons Attribution (CC BY) license (https://creativecommons.org/licenses/by/4.0/).

1. Introduction

The rising penetration of distributed generation (DG), renewable energy, and power electronic devices has fundamentally transformed existing distribution networks. Distribution networks are no longer radial feeders operated passively; they must now handle bidirectional power flows, suppress voltage fluctuations, and reduce losses with highly

dynamic loading and generation profiles. This presents challenges, requiring advanced optimization schemes capable of ensuring reliability, efficiency, and scalability.

Distribution Network Reconfiguration (DNR) has been confirmed as an effective tool to reduce real power losses and strengthen voltage stability by switching the open/closed positions of sectionalizing and tie switches. Research has verified its suitability when coupled with distributed generation, capacitor allocation, or with other adaptable devices [1–3]. Coupling with renewable-based DG and compensators also makes the grid more efficient, with better voltage profiles and reduced network congestion [2–4]. Multi-objective formulations of the DNR problem capture the trade-offs between loss minimization, voltage profile improvement, and device utilization [5,6].

As the DNR problem is a significant nonlinear and combinatorial optimization problem, there have been extensive applications of metaheuristic algorithms. Classical algorithms, such as Particle Swarm Optimization (PSO), Genetic Algorithms (GA), Ant Colony Optimization (ACO), and Tabu Search [7–9], are established but have the tendency to converge too early, with high parameter sensitivity. To address these issues, many nature-inspired and swarm-based methods have been proposed, including the Grey Wolf Optimizer (GWO) [1,5], Harris Hawks Optimization (HHO) [10], Equilibrium Optimizer (EO) [11], Atom Search Optimization (ASO) [12], Pigeon-Inspired Optimization (PIO) [13], the Grasshopper Optimization Algorithm (GOA) [14], and the Flower Pollination Algorithm (FPA) [15]. Comparative studies confirm that these methods generally outperform conventional algorithms, though each has specific strengths and weaknesses [16–18]. Even so, significant challenges persist. Most algorithms are trapped in local optima, sensitive to parameter tuning, or do not scale well when applied to large distribution networks [7,19]. Summaries of current methodologies reveal inadequacies in resisting stochastic renewable generation, time-varying loads, and protection constraints [20–22]. Moreover, the great majority of methodologies presume set network data, and scarce comprehensive large-scale benchmarks render systematic comparisons difficult [19]. These challenges indicate the value of more adaptive, hybrid, and scalable optimization platforms.

In addition to reconfiguration, a potential way to raise the flexibility of distribution networks is through integration with Soft Open Points (SOPs). Installed with back-to-back voltage source converters, SOPs offer active and reactive power transfers between feeders in a controlled manner, with abilities far exceeding those of tie switches in the traditional sense. If properly integrated with DNR, SOPs have been found to reduce losses substantially, tighten voltage profiles, and raise system reliability. But integration comes with an otherwise nontrivial mixed-integer nonlinear programming (MINLP) problem, characterized by high-dimensional search spaces, nonlinear power flow constraints, and tight operating limits on devices [23]. Typical algorithms find it inefficient to handle such complexity, especially in larger networks [24].

Recent work emphasizes that hybridization of metaheuristics decreases premature convergence and balances global exploration and local exploitation [12,15,16,18]. Additionally, better formulations indicate additional challenges related to scalability, management of uncertainty, and synchronizing SOPs, with protection schemes and dynamic stability requirements [23,25]. These gaps provide strong motivation for the development of more robust and flexible optimization methods tailored to SOP-integrated distribution systems. Although hybridization is an accepted approach to improve metaheuristic performance, the hybrid structure has a determining effect on its efficiency. Numerous current hybrid methodologies, like PSO–GWO [26] and hPSO-TLBO [27], utilize a cascaded or sequential framework in which one algorithm is applied sequentially following another in a predetermined style. By contrast, the new hTLBO–CO algorithm presents a parallel-cooperative hybridization architecture. Here, the TLBO Teacher Phase (exploitation with focus), the

CO Hunting Phase (intelligent exploration), and the TLBO Learner Phase (social learning) operate concurrently on dynamically partitioned sub-populations. One of the innovations is the shared elite pool, which facilitates continuous, two-way information exchange among all three phases. This structure facilitates adaptive resource allocation based on real-time feedback on performance to realize a more dynamic and resilient balance between global exploration and local exploitation than with sequential hybrids. This parallel cooperative strategy is one of the central conceptual and structural advancements of our approach.

To overcome these limitations, in this paper, a hybrid Teaching–Learning-Based Optimization and Cheetah Optimizer (hTLBO–CO) for SOP-integrated distribution network reconfiguration is put forward. The main benefits and novelty of the proposed framework over existing models are multi-faceted, addressing many key issues in the field:

- One of the major issues in the field is the premature convergence problem of metaheuristic algorithms in the high-dimensional, non-convex search space. The proposed hTLBO–CO introduces a critical architectural novelty through its parallel cooperative architecture. Unlike sequential hybrids, this approach enables concurrent execution of specialized search phases—TLBO for exploitation [27], CO for exploration [28], and a social learning phase—supported by a collaborative knowledge repository. This arrangement enables continuous, bidirectional information sharing and dynamic resource pooling, effectively resolving premature convergence and stagnation issues affecting other solvers.
- The existing models are likely to lack effectiveness in modeling the realistic integration of SOPs. The new formulation takes a significant step by allowing the adaptive placement of SOPs on a wider range of network switches, thereby expanding the network of feasible solutions. A principal innovation is the introduction of a new topological compatibility constraint, one that systematically captures the important physical requirement that an SOP must be installed in an open branch. This ensures that all solutions derived are topologically correct and physically viable, which counteracts the prevalent source of infeasibility in other approaches.
- Moving beyond standard single-objective optimization, this work introduces an entire multi-objective analysis that precisely quantifies the trade-offs between key performance metrics, such as power loss, voltage profile, and capital expenditure. This offers system planners a robust decision-making framework. Moreover, the demonstrated performance excellence is tightly supported by extensive statistical testing and provides high confidence in the algorithm's robustness and reliability across various independent runs.
- Computational intractability of the underlying problem for large-scale networks is a main practical hindrance. The design of the framework involves an evolved multistage approach to dealing with sophisticated constraints and computational acceleration algorithms. This integrated solution confronts the scalability challenge head-on, enabling efficient optimization of realistically scaled distribution networks, where conventional methods typically become ineffective or fail.

Briefly, this paper's main contributions are as follows:

- A novel hTLBO–CO hybrid algorithm with a parallel cooperative design.
- A comprehensive mathematical model with an innovative topological compatibility constraint.
- A robust constraint-handling and computational strategy for scalability.
- Extensive validation, such as multi-objective Pareto analysis and statistical significance testing, to demonstrate consistent supremacy.

The remainder of the paper is organized as follows: Section 2 describes the mathematical modeling of the SOP-integrated network reconfiguration problem. Section 3 presents the hTLBO-CO algorithm. Section 4 provides the implementation platform of combining the optimizer with the power grid model. Section 5 offers simulation results and discussions on IEEE test networks with comparisons with other algorithms. Finally, Section 6 concludes the paper, with significant contributions and future research directions.

2. Mathematical Formulation of SOP-Integrated Network Reconfiguration

The addition of SOPs to distribution networks creates an intimidating MINLP challenge, requiring a vigorous mathematical expression to effectively capture the coupling between discrete switching actions, SOP location decisions, and continuous power flow variables. This section presents an overall mathematical model of the SOP-integrated distribution network reconfiguration challenge, which is posed as an optimization problem with the objective of minimizing total active power losses subject to operational, topological, and device-specific constraints. The formulation formally allows for SOP installation on tie and sectionalizing switches, adds a novel topological compatibility constraint to ensure physical realizability, and specifies the ensuing high-dimensional, nonconvex solution set to pave the way towards the application of the proposed hybrid optimization scheme.

2.1. Objective Function

The goal of optimization is to reduce overall active power losses of the distribution system through coordinated control of SOPs and network reconfiguration [29]:

$$\min P_{\text{loss}}^{\text{total}} = \sum_{b=1}^{N_b} x_b R_b \frac{P_b^2 + Q_b^2}{|V_b|^2} \tag{1}$$

where $P_{\text{loss}}^{\text{total}}$ represents total system power losses, N_b is the total number of branches, R_b denotes branch resistance, P_b and Q_b are active and reactive power flows in branch b, and $|V_b|$ is the voltage magnitude at the sending node of branch b. $x_b \in \{0,1\}$ indicates the operational status (1: closed, 0: open) of the b-th branch. This expression of quadratic loss integrates conductor heat losses and the losses of the transformer's copper, with the results being a nonconvex optimization environment highly susceptible to reactive power flows with SOP operation.

2.2. Decision Vector Construction

The joint optimization of switch states, SOP placements, and power injections is encoded in the decision vector:

$$X = [\underbrace{x_1, \ldots, x_{N_{\text{sw}}}}_{\mathcal{S}_{\text{sw}}}, \underbrace{z_1, \ldots, z_M}_{\mathcal{L}_{\text{SOP}}}, \underbrace{P_{\text{SOP}}^1, Q_{\text{SOP}}^1, \ldots, P_{\text{SOP}}^M, Q_{\text{SOP}}^M}_{\mathcal{P}_{\text{SOP}}}] \tag{2}$$

where $\mathcal{S}_{\text{sw}}$ represents the switch state subspace with $x_i \in \{0,1\}$, indicating the operational status (1: closed, 0: open) of the i-th switch in the set of N_{sw} switches; $\mathcal{L}_{\text{SOP}}$ denotes the SOP location subspace, where $z_j \in \{0,1\}$ determines whether an SOP is installed at candidate branch j from M eligible branches ($M \leq N_{\text{sw}}$); and $\mathcal{P}_{\text{SOP}}$ constitutes the continuous power injection subspace, with $\left(P_{\text{SOP}}^j, Q_{\text{SOP}}^j\right) \in \mathbb{R}^4$ specifying the active and reactive power injections for the SOP at branch j (sending-end and receiving-end nodes of the branch).

2.3. Constraints

2.3.1. SOP Operational Constraints

Each SOP unit's operating limit should be enforced according to the unit's installation [30]. This can be achieved by correlating the continuous power variables with the binary location variable z_j. The constraints should also consider the power flow through the SOP branch's both terminal nodes.

For a potential branch $j \in \{1, \ldots, M\}$ in which an SOP could be installed:

1. Capacity Constraint (at both terminals): The apparent power entering or leaving both the receiving-end (r) and sending-end (s) nodes of the SOP must not exceed its rated capacity in case the SOP is active ($z_j = 1$). If SOP does not exist ($z_j = 0$), then power injections are all zeros.

$$\sqrt{\left(P^j_{SOP,s}\right)^2 + \left(Q^j_{SOP,s}\right)^2} \leq z_j \cdot S^j_{\text{rated}} \tag{3}$$

$$\sqrt{\left(P^j_{SOP,r}\right)^2 + \left(Q^j_{SOP,r}\right)^2} \leq z_j \cdot S^j_{\text{rated}} \tag{4}$$

where $P^j_{SOP,s}$ and $Q^j_{SOP,s}$ are the active and reactive power injections at the sending-end node of branch j, $P^j_{SOP,r}$ and $Q^j_{SOP,r}$ are the injections at the receiving-end node, and S^j_{rated} is the rated capacity.

2. Active Power Coupling Constraint: For a lossless SOP connecting branch j across nodes s and r, active power injection in node s must be equal to the negative of injection in node r with a net active power exchange of zero [30].

$$P^j_{SOP,s} + P^j_{SOP,r} = 0 \tag{5}$$

3. Reactive Power Independence: The reactive power of each terminal can be separately adjusted within the capability of the device, subject to the constraints in (3) and (4).

$$Q^j_{SOP,s}, Q^j_{SOP,r} \in \left[-z_j \cdot S^j_{\text{rated}},\ z_j \cdot S^j_{\text{rated}}\right] \tag{6}$$

This expression ensures that if $z_j = 0$, then power injections are set to zero, effectively disabling the SOP of the branch. The binary variable z_j adequately scales the operational feasible region.

2.3.2. Voltage Constraints

Bus voltage magnitudes must remain within statutory limits:

$$V_{\min} \leq |V_i| \leq V_{\max}\ \forall i \in \{1, \ldots, N_{\text{bus}}\} \tag{7}$$

Typically, $V_{\min} = 0.95$ pu and $V_{\max} = 1.05$ pu.

2.3.3. Topological Constraints

Network reconfiguration must maintain radial structure:

$$\sum_{i=1}^{N_{\text{sw}}} x_i = N_{\text{bus}} - N_{\text{sub}} - 1 \tag{8}$$

where N_{sub} is the number of substations. This ensures exactly $N_{\text{bus}} - N_{\text{sub}} - 1$ closed switches, forming a spanning tree without loops.

2.3.4. Switch Status Constraints

Each switch position is binary-constrained:

$$x_i \in \{0,1\}\ \forall i \in \{1,\ldots,N_{\text{sw}}\} \tag{9}$$

Practical implementation requires additional feeder connectivity constraints to avoid network fragmentation.

2.3.5. SOP Installation Constraints

The number of installed SOPs is constrained by the budgetary limit N_s:

$$\sum_{j=1}^{M} z_j = N_s \tag{10}$$

This cardinality restriction ensures the solution remains within feasible implementation limitations.

2.3.6. Topological Compatibility

The interaction between SOP placement and switch states is governed by

$$z_j \leq 1 - x_j\ \forall j \in \{1,\ldots,M\} \tag{11}$$

This inequality enforces the fundamental necessary condition that an SOP should be installed on an open branch. The constraint results from the physical reality that SOPs require electrical isolation from the main network so they can act as controlled voltage sources.

2.4. Solution Space Characterization

The complete solution space $\mathcal{X}$ is the Cartesian product:

$$\mathcal{X} = \{0,1\}^{N_{\text{sw}}+M} \times \mathbb{R}^{4M} \tag{12}$$

subject to constraints (2)–(11). This space has

- A combinatorial component with $2^{N_{\text{sw}}+M}$ possible configurations;
- A continuous component, forming a $4M$-dimensional polytope bounded by the SOP capacity constraints.

2.5. Computational Complexity Analysis

The problem belongs to the MINLP class, with

$$\mathcal{O}\left(2^{N_{\text{sw}}+M} \times \mathcal{F}(4M)\right) \tag{13}$$

in which $\mathcal{F}(4M)$ represents the size of the continuous power flow problem with $4M$ variables. The exponential is based on the binary decisions, and $\mathcal{F}(4M)$ typically scales polynomially with network size.

3. Proposed Hybrid TLBO-CO Algorithm

3.1. Algorithm Overview

This paper introduces a novel hybrid optimization algorithm that synergistically blends the Teaching–Learning-Based Optimization (TLBO) [27] and the Cheetah Optimizer (CO) [28] metaheuristics. The novel hTLBO-CO algorithm has been specifically developed to cope with the shortcomings of single algorithms while resolving the high-dimensional, generally non-convex, and complex optimization problems prevalent in present-day power systems.

As demonstrated in Figure 1, the structure of the algorithm consists of three parallel optimization streams, each with a distinct search behavior, while concurrently engaging in continual, coordinated information sharing. The TLBO Teacher Phase provides specialized exploitation with gradient-informed mechanisms to refine solution quality in promising areas. Meanwhile, the CO Hunting Phase induces intelligent exploration with biological motifs, vigorously sieving through the search territory for new optima. A joint elite pool acts as an anchor knowledge repository, facilitating dynamic information sharing amongst these phases. This pool is moderated with a crowding distance criterion to ensure population diversity and prevent premature convergence. This dual process of competitive exclusion and cooperative learning ensures an effective balance between global exploration potential and local exploitative precision.

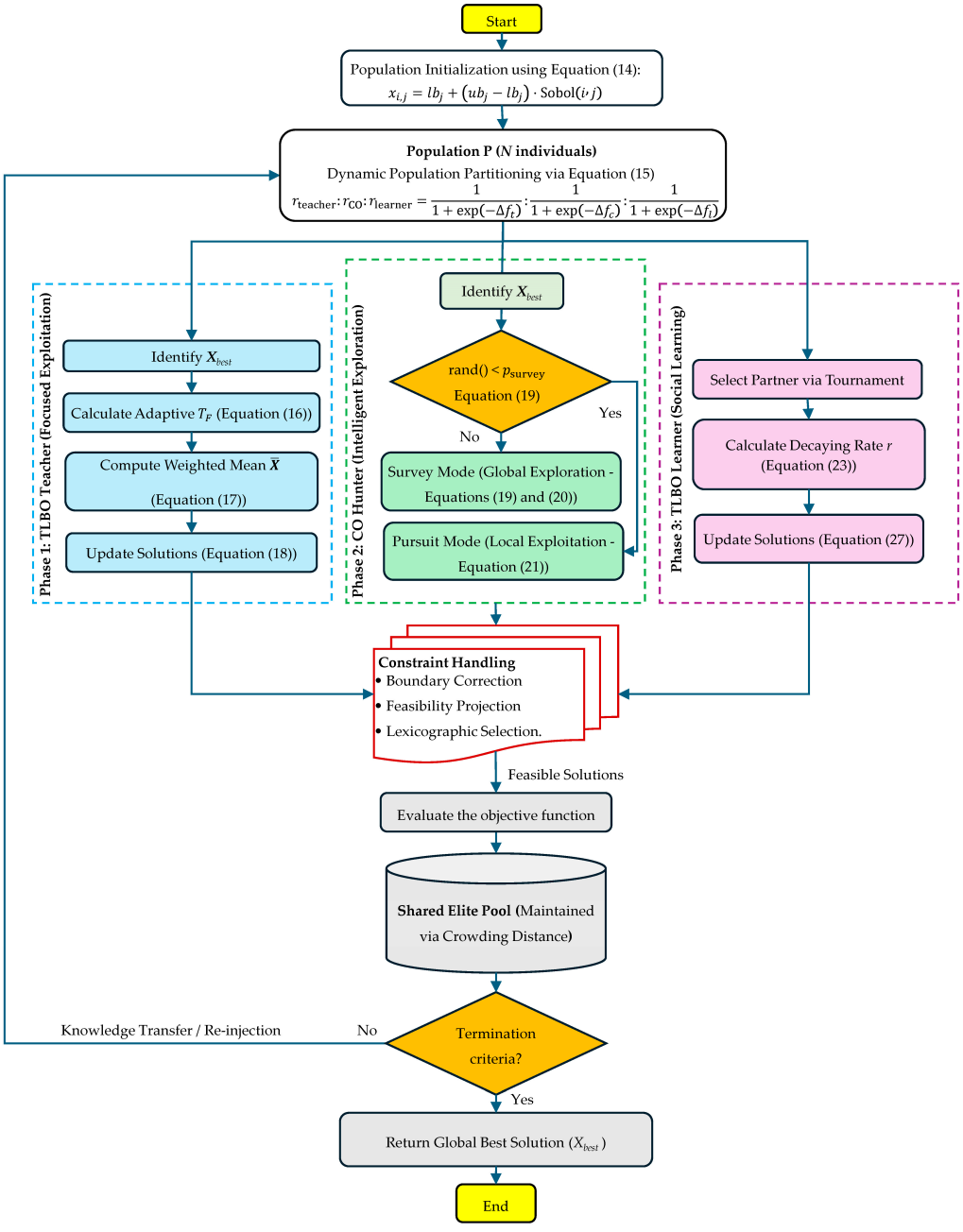


Figure 1. High-level architecture and dataflow of the proposed hTLBO-CO algorithm.

3.2. Population Initialization and Management

Superior initialization is critical for successful optimization of high-dimensional landscapes. The existing method employs quasi-random Sobol sequences to produce a more full and uniform coverage of the feasible search area compared with standard pseudo-random number generators.

The population, or **P**, is made up of N candidate solutions (i.e., "individuals"). Each individual $\boldsymbol{X}_i$ is a D-dimensional vector comprising a potential solution to the optimization problem, $\boldsymbol{X}_i = (x_{i,1},\ x_{i,2},\ \ldots,\ x_{i,D})$, with D being the number of decision variables. Lower and upper bounds on variable j are provided by lb_j and ub_j, respectively.

For each variable j in individual i, the initialization is defined as

$$x_{i,j} = lb_j + \left(ub_j - lb_j\right) \cdot \mathrm{Sobol}(i,j) \tag{14}$$

with the deterministic "Sobol(*i*,*j*)" function returning the j-th component of the i-th Sobol sequence point, with low-discrepancy sampling.

The sub-populations $\mathbf{P_1}$ (Teacher Phase), $\mathbf{P_2}$ (CO Phase), and $\mathbf{P_3}$ (Learner Phase) are split adaptively from the population **P** dynamically. The adaptive split ratios r_{teacher}, r_{CO}, and r_{learner} are computed from a sigmoidal scaling function:

$$r_{\text{teacher}} : r_{\text{CO}} : r_{\text{learner}} = \frac{1}{1+\exp(-\Delta f_t)} : \frac{1}{1+\exp(-\Delta f_c)} : \frac{1}{1+\exp(-\Delta f_l)} \tag{15}$$

Δf_t, Δf_c, and Δf_l here are exponential moving averages of the fitness enhancements registered during their respective phases during the previous iteration time window. This expression allows for smooth transitions from exploration-prevalent configurations to exploitation-prevalent ones, while also making all phases participate with a minimum level necessary to achieve algorithmic stability.

3.3. TLBO Teacher Phase (Focused Exploitation)

The Teacher Phase is supplemented with several high-level refinements. The teacher factor T_F ceases to be a random variable but changes over time following a logistic growth curve to monitor the convergence state of the population:

$$T_F = 1 + \frac{1}{1+\exp(-k(t-t_0))} \tag{16}$$

where t represents the number of iterations running right now, k is an adaptation rate-controlling constant, and t_0 is a reference iteration corresponding to the moment when significant population diversity decreases. Next, the mean position of the class $\overline{\boldsymbol{X}}$ is calculated with a fitness-weighted values:

$$\overline{\boldsymbol{X}} = \frac{\sum_{i=1}^{N_1} w_i \boldsymbol{X_i}}{\sum_{i=1}^{N_1} w_i},\ w_i = \frac{1}{1+f(\boldsymbol{X_i}) - f_{\min}} \tag{17}$$

where N_1 is the size of sub-population $\mathbf{P_1}$, $f(\boldsymbol{X_i})$ is the fitness of individual i, and $f_{\min}$ is the best fitness found in $\mathbf{P_1}$. Third, the solution update rule is augmented with a momentum term $\boldsymbol{v}_{\mathbf{prev}}$ (the previous update vector for $\boldsymbol{X_i}$ to stabilize the search trajectory:

$$\boldsymbol{X}_{i,\text{new}} = \boldsymbol{X}_i + \beta \boldsymbol{v}_{\mathbf{prev}} + (1-\beta) r_1 \left(\boldsymbol{X}_{best} - T_F \overline{\boldsymbol{X}}\right) \tag{18}$$

where β is a momentum coefficient, r_1 is a random vector uniformly distributed in [0, 1], and $\boldsymbol{X}_{best}$ is the best solution identified (the "teacher").

3.4. CO Hunting Phase (Intelligent Exploration)

The CO Phase emulates the cheetah's hunting style with dual modes. In *Survey Mode*, solutions execute global exploration with anisotropic Gaussian mutations, whose covariance matrix $\mathbf{\Sigma}$ is updated according to the current distribution of the population:

$$\boldsymbol{X}_{i,\text{new}} = \boldsymbol{X}_i + \sigma_t \mathcal{N}(\mathbf{0}, \mathbf{\Sigma})(\boldsymbol{X}_{best} - \boldsymbol{X}_i) \tag{19}$$

$$\Sigma_{jj} = \frac{1}{N} \sum_{i=1}^{N} \left(x_{i,j} - \overline{x}_j \right)^2 \tag{20}$$

where $\mathcal{N}(\mathbf{0}, \mathbf{\Sigma})$ is a Gaussian vector of random numbers with mean 0 and covariance $\mathbf{\Sigma}$, σ_t is a step size parameter that decreases with time, and $\overline{x}_j$ is the arithmetic mean of the j-th variable over the entire population. This adaptation focuses exploration on non-converged dimensions.

Pursuit Mode solutions carry out direction-based local exploitation, with their search centered around the best possible improvement directions:

$$\boldsymbol{X}_{i,\text{new}} = \boldsymbol{X}_{best} + \alpha \boldsymbol{\mathcal{D}}(\theta),\ \theta \sim \text{vMF}(\kappa) \tag{21}$$

where α is a step size, and direction vector $\boldsymbol{\mathcal{D}}(\theta)$ is sampled from a von Mises–Fisher distribution vMF(κ) with concentration parameter κ, ensuring that perturbations are focused around the direction toward the best current solution $\boldsymbol{X}_{best}$.

The running probability in survey mode p_{survey} is high initially to encourage exploration and then decreases linearly during optimization:

$$p_{\text{survey}} = 0.5 + 0.4 \left(1 - \frac{t}{t_{\max}} \right) \tag{22}$$

where $t_{\max}$ is the maximum number of iterations. This probability is then set back to a high value when a new global best solution is discovered to encourage exploration of promising new regions.

3.5. TLBO Learner Phase (Social Learning)

The learner phase provides social learning through peer-to-peer interactions. Primary enhancements include a tournament-based partner selection scheme, which exerts controlled selection pressure. Moreover, the learning rate r decreases exponentially with time so that convergence stability is approached in the latter phase of optimization:

$$r = r_0 \cdot \exp(-\lambda t) \tag{23}$$

where r_0 is the initial learning rate, and λ is the decay constant. The update direction for a learner $\boldsymbol{X}_i$ interacting with a partner $\boldsymbol{X}_j$ is a hybrid strategy:

$$\boldsymbol{X}_{\text{new}} = \boldsymbol{X}_i + r\left[\gamma(\boldsymbol{X}_i - \boldsymbol{X}_j) + (1-\gamma)\boldsymbol{d}_{\text{prev}}\right] \tag{24}$$

where $\gamma \in [0,\ 1]$ is a weighting factor, and $\boldsymbol{d}_{\text{prev}}$ is a direction vector from the cumulative past successful updates of $\boldsymbol{X}_i$. This approach balances social learning's benefits with the counsel of collective search experience.

3.6. Constraint Handling

The proposed approach uses a robust three-stage planning method to efficiently address constraints.

1. Boundary Correction: Values out of variable bounds are set through component-wise clamping: $x_{i,j} = max\big(lb_j, min\big(ub_j, x_{i,j}\big)\big)$.
2. Feasibility Projection: Infeasible solutions of nonlinear constraints are projected onto the set $\mathcal{F}$ of feasible solutions by

$$\boldsymbol{X}_{\text{feas}} = \arg\min_{\boldsymbol{X}' \in \mathcal{F}} \| \boldsymbol{X} - \boldsymbol{X}' \|_2 \tag{25}$$

   This is accomplished through an efficient active-set method.
3. Lexicographic Selection: A feasibility-first rule is imposed during selection, ensuring that the algorithm always prefers and converges towards feasible regions.

3.7. Computational Complexity

The hTLBO-CO algorithm is also computationally efficient. Per-iteration complexity is linear with respect to the population size N and problem dimension D. The main components consist of the evaluation of fitness (which is assumed to take $\mathcal{O}(D)$) and update operations in each of the three phases, each with a size of ~$N/3$:

$$\mathcal{O}(N \cdot D) + \mathcal{O}(D^2)_{\text{covariance}} \tag{26}$$

The $\mathcal{O}\big(D^2\big)$ term, arising from the calculation of the covariance matrix $\boldsymbol{\Sigma}$ in the CO phase (Equation (20)), becomes negligible for high-dimensional problems (typically $D > 100$), confirming the scalability of the proposed approach. This complexity is competitive with and often more efficient than other algorithms, like PSO ($\mathcal{O}(N \cdot D)$) and GA ($\mathcal{O}(N \cdot D) + \mathcal{O}(N\log N)$), for large-scale problems.

3.8. Convergence Analysis

The hTLBO-CO hybrid architecture provides a background of stable global convergence. The behavior of the algorithms can be described as a finite Markov chain, where the phases of TLBO maintain elitism through their transitions, and the phases of CO meet the required constraints to support ergodicity through their non-zero exploration probabilities:

$$\lim_{t \to \infty} P(\boldsymbol{X}_t \in \boldsymbol{\mathcal{X}}^*) = 1 \tag{27}$$

where $\boldsymbol{\mathcal{X}}^*$ represents the set of global optima. This theoretical guarantee of asymptotic convergence is supported by extensive empirical validation on standard benchmark suites.

The core of the proposed hybridization strategy is a dynamic population partitioning and shared elite pool framework. The population is adaptively split into three subpopulations for the TLBO Teacher Phase (focused exploitation), the CO Hunting Phase (intelligent exploration), and the TLBO Learner Phase (social learning), with the split ratios $(r_{teacher}, r_{CO}, r_{learner})$ being dynamically adjusted based on the recent performance of each phase (Equation (15)).

The crucial element for information exchange is the joint elite pool, which acts as a central knowledge repository. This pool is continuously updated with the best solutions from all three phases and maintained using a crowding distance criterion to ensure diversity. The elite pool is not passive; it actively facilitates information exchange in two ways:

- It provides the global best solution ($\mathbf{X}_{best}$) that guides the update equations in both the Teacher Phase (Equation (18)) and the CO's pursuit mode (Equation (21));
- It serves as a source for re-injecting high-quality, diverse solutions back into the sub-populations, preventing stagnation and fostering cooperative learning.

This architecture ensures that exploitative refinements from TLBO and exploratory discoveries from CO are continuously shared, creating a synergistic effect that is more powerful than the sum of its parts.

The pseudocode of the proposed hTLBO-CO algorithm is presented in Algorithm 1.

Algorithm 1: Pseudocode of the hTLBO-CO algorithm

Input: Population Size N, Max Iterations t_{max}, Lower Bounds lb, Upper Bounds ub
Output: Best solution X_{best}

Initialize population $\mathbf{P}$ of size N using Equation (14)//Section 3.2
Evaluate fitness $f(\boldsymbol{X})$ for all individuals $\boldsymbol{X} \in \mathbf{P}$
$X_{best} \leftarrow$ argmin_{$\boldsymbol{X} \in \mathbf{P}$} $f(\boldsymbol{X})$
for iteration $t = 1$ to t_{max} **do**
    Partition P into $\mathbf{P_1}$, $\mathbf{P_2}$, $\mathbf{P_3}$ using ratios from Equation (15)//Section 3.2

    % Phase 1: TLBO Teacher Phase ($\mathbf{P_1}$- Exploitation)
    for each individual $\boldsymbol{X}_i$ in sub-population $\mathbf{P_1}$ **do**
        Calculate adaptive T_F (Equation (16))
        Calculate fitness-weighted mean $\overline{\boldsymbol{X}}$ (Equation (17))
        Update solution: $\boldsymbol{X}_{i,\text{new}} \leftarrow$ Apply Equation (18)
        Enforce constraints on $\boldsymbol{X}_{i,\text{new}}$ (Section 3.6)
        Evaluate $f(\boldsymbol{X}_{i,\text{new}})$ and update $\boldsymbol{X}_i$ if improved
    end for

    % Phase 2: CO Hunting Phase ($\mathbf{P_2}$- Exploration)
    Calculate current survey probability p_{survey} (Equation (22))
    for each individual $\boldsymbol{X}_i$ in sub-population $\mathbf{P_2}$ **do**
        if rand() < p_{survey} **then**
            Update via Survey Mode: $\boldsymbol{X}_{i,\text{new}} \leftarrow$ Apply Equations (19) and (20)
        else
            Update via Pursuit Mode: $\boldsymbol{X}_{i,\text{new}} \leftarrow$ Apply Equation. (21)
        end if
        Enforce constraints on $\boldsymbol{X}_{i,\text{new}}$ (Section 3.6)
        Evaluate $f(\boldsymbol{X}_{i,\text{new}})$ and update $\boldsymbol{X}_i$ if improved
    end for

    % Phase 3: TLBO Learner Phase ($\mathbf{P_3}$—Social Learning)
    Calculate current learning rate r (Equation (23))
    for each individual $\boldsymbol{X}_i$ in sub-population $\mathbf{P_3}$ **do**
        Randomly select a partner $\boldsymbol{X}_j$ from $\mathbf{P}$ ($j \neq i$) via tournament selection
        Update solution: $\boldsymbol{X}_{i,\text{new}} \leftarrow$ Apply Equation (24)
        Enforce constraints on $\boldsymbol{X}_{i,\text{new}}$ (Section 3.6)
        Evaluate $f(\boldsymbol{X}_{i,\text{new}})$ and update $\boldsymbol{X}_i$ if improved
    end for

    Update the best global solution: $X_{best} \leftarrow$ argmin($f(X_{best})$, min_{$\boldsymbol{X} \in \mathbf{P}$} $f(\boldsymbol{X})$)
    Update moving averages Δf_t, Δf_c, and Δf_l for adaptive ratios (Equation (15))
end for
Return X_{best}

4. Implementation Framework for SOP-Integrated Reconfiguration

This section presents the entire computational framework developed to integrate the proposed hTLBO-CO algorithm into the complex MINLP problem of simultaneous DNR and SOP optimization. The framework should efficiently handle the mixed-variable decision space, enforce strong operational constraints, and hasten the optimization process feasible for practical, large-scale implementations.

4.1. Algorithmic Integration with Power System Model

The interaction of the power system model with the hTLBO-CO optimizer is controlled through three dedicated, coupled modules, given in Figure 2:

- Topology Decoder ($\mathcal{M}_1$): This module translates the binary part of the decision vector $\boldsymbol{X}$ (switch state x_i and SOP placement flags z_j) to a valid radial network topology. This module constructs the network graph G_t associated with iteration t with primitives of graph theory:

$$G_t = (V, E_t) \text{ where } E_t = \{e_b | x_i = 1 \text{ for switch } i \text{ controlling branch } b\} \quad (28)$$

  Here, V is the set of buses (nodes) and E_t is the set of energized branches (edges) determined by the closed switches.
- SOP Controller ($\mathcal{M}_2$): This module is responsible for the continuous part of X, which computes the active and reactive power setpoints ($P^j_{\text{SOP}}, Q^j_{\text{SOP}}$) of every installed SOP. It also ensures the setpoints are within the operating envelope of the device prior to presenting them to the power flow solver.
- Power Flow Validator ($\mathcal{M}_3$): This is the principal computational engine that assesses the efficiency and feasibility of a possible solution. It calculates the power flow equations of the topology input provided from $\mathcal{M}_1$ with the SOP injections from $\mathcal{M}_2$ to determine the bus voltages, branch flows, and total power loss. It also checks for constraint violations.

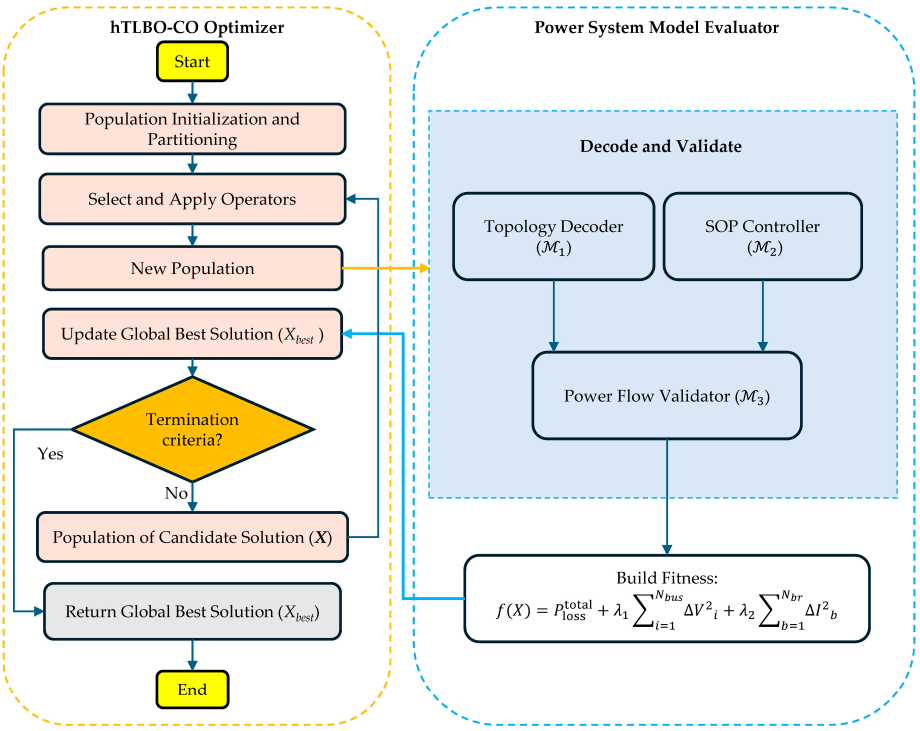


Figure 2. Workflow of the hTLBO-CO optimization framework, showing the interaction between the algorithm and the power system model for evaluating candidate solutions.

In the iterative process shown in Figure 2, the hTLBO-CO optimizer generates potential solutions ($\boldsymbol{X}$). Each solution is decoded and verified via the system modules, and the produced value of fitness—power loss with penalty adaptations—is sent back to the optimizer to guide the next generation.

4.2. Solution Representation and Initialization

A possible solution $\boldsymbol{X}_k$ of the integrated problem is a compound vector with discrete (binary) and continuous (real-valued) variables:

$$\boldsymbol{X}_k = \left[\underbrace{x_1, \ldots, x_{N_{sw}}}_{\text{Switches}}, \underbrace{z_1, \ldots, z_M}_{\text{SOPlocations}}, \underbrace{P^1, \ldots, P^M, Q^1, \ldots, Q^M}_{\text{SOPinjections}} \right] \tag{29}$$

For attaining a high-quality and diversified initial population, a methodically initialized technique is applied:

- Switch States (x_i): Initialized via a Bernoulli distribution, $x_i^{(0)} \sim \text{Bernoulli}(0.5)$, to randomly generate radial configurations.
- SOP Placement (z_j): Set with an initially biased Bernoulli distribution, $z_j^{(0)} \sim \text{Bernoulli}(\min(0.2, N_s/M))$, to encourage diversity while being respectful of the constraints.
- SOP Power Setpoints ($P^j_{\text{SOP}}, Q^j_{\text{SOP}}$): Initialized with a uniform distribution within their operational limits, $P^j_{\text{SOP}}, Q^j_{\text{SOP}} \sim \mathcal{U}\left(-S^j_{\text{rated}},\ S^j_{\text{rated}}\right)$.

This mixed initialization scheme, combined with the use of Sobol sequences in the continuous components, assures comprehensive coverage of the complex search space provided in Equation (14).

4.3. Constraint Handling Mechanism

A robust multi-level strategy is required to address the numerous constraints efficiently.

- Topological Feasibility: Radiality constraints are enforced through

$$\text{rank}(\mathbf{A}(G_t)) = N_{\text{bus}} - N_{\text{sub}} - 1 \tag{30}$$

where $\boldsymbol{A}$ represents the incidence matrix. If a solution violates radiality, then a repair mechanism is initiated with the help of an MST algorithm:

$$G_{t'} = \text{Minimum Spanning Tree } (G_t, w_b = R_b) \tag{31}$$

The MST uses branch resistances R_b as edge weights to compute the radial topology with the least possible resist losses while preserving connectivity, restoring the solution.

- SOP-Placement Coupling: The logical constraint $z_j \leq 1 - x_j$ (meaning an SOP can only be placed onto an open branch) is enforced directly in the following solution representation:

$$z_j = \min\left(z_j, 1 - x_j\right)\ \forall j \tag{32}$$

This basic projection guarantees feasibility without substantially altering the optimizer's direction of search.

- Power Flow and Device Constraints: The power flow checker checks violations of voltage constraints ($|V_i| \in [0.95, 1.05]$ pu) and branch current constraints ($\left|I_b\right| \leq I_b^{\max}$).

SOP capacity constraints are enforced via a direct projection of their power setpoints onto the feasible circle defined by S^j_{rated}:

$$(P^j, Q^j) \leftarrow \frac{(P^j, Q^j)}{\max\left(1, \| (P^j, Q^j) \|_2 / S^j_{\max}\right)} \tag{33}$$

- Penalty Function: Infeasible solutions corresponding to violation of the soft constraints (e.g., voltage limit violations) are penalized but not eliminated to steer the search towards feasible regions again. The fitness function becomes

$$f(X) = P^{\text{total}}_{\text{loss}} + \lambda_1 \sum_{i=1}^{N_{bus}} \Delta V^2{}_i + \lambda_2 \sum_{b=1}^{N_{br}} \Delta I^2{}_b \tag{34}$$

where ΔV_i and ΔI_b are the magnitudes of voltage and current limit violations, respectively, and λ_1 and λ_2 are large penalty coefficients.

4.4. Fitness Evaluation Pipeline

Validation of a solution's potential is subject to a strict, multi-stage pipeline to ensure precision and effectiveness:

- Topology Validation and Repair: The switch states are decoded to a graph G_t. If non-radial, then MST repair is applied.
- SOP Activation: The power injections corresponding to every unplaced SOP (z_j) are initialized to zero.
- Power Flow Solution: A balanced three-phase power flow is solved using a current injection method, which is also effective for radial distribution networks.
- Loss Computation: The overall power loss $P^{\text{total}}_{\text{loss}}$ is determined from branch flows.
- Application of Penalty: All remaining constraint violations' penalty terms are added to the loss value to obtain the final fitness $f(X)$.

4.5. Solution Evaluation and Iterative Convergence

While the above sections explain the internal operation of the hTLBO-CO algorithm, this subsection describes the closed-loop evaluation process responsible for steering the system to an optimal solution. The effectiveness of the algorithm is not merely due to its searching policy but also due to the robust feedback mechanism evaluating and selecting possible designs.

This iterative flow depicts a dynamic evaluation cycle. The set of candidate solutions ($\boldsymbol{X}$) from the core of the hTLBO-CO is more than a set of parameter values. Each individual solution is decoded and validated in order to transform it back into a feasible, constraint-satisfying design, which is a critical step for abstract numerical representations.

The generated numerical value of the fitness, given as the total power loss with the inclusion of penalty terms for constraints, becomes the ultimate measure of performance. This measure is critical because it balances the main goal (minimizing power loss) with the implementation ability of the solution in practice. Through the direct inclusion of penalties in the fitness function, the search process naturally avoids the infeasible areas of the solution set.

This evaluation score is then returned to the optimizer, marking the end of the feedback cycle. It is with this continual data stream of evaluation data that the hTLBO-CO gains insight from one succeeding generation to the next, all while refining the population. Convergence of the algorithm is consequently not a predetermined sequence but an adaptive measure in response to the quality of solutions being taken during such a cycle. Section 4.6

presents a numerical study of the convergence behavior and the final optimized results determined through such a process.

4.6. Computational Acceleration Techniques

To render the optimization tractable at a large-system scale, three principal acceleration methodologies are used:

- Topology Catching: Radiality status and power flow outcomes of frequent switch configurations are saved in a hash-map to avoid redundant calculation.
- Warm Starts: The power flow solver is initialized with the last evaluation's corresponding topology voltage profile, significantly reducing the number of iterations required to converge.
- Parallel Assessment: The assessment of the fitness of the population is divided across many CPU cores since these assessments do not occur sequentially but are independent of each other. This leads to almost linear speedup with the number of cores present.

4.7. Convergence Monitoring

The algorithm monitors three quantities in order to assess convergence and termination:

- Centroid Motion (γ_1): Assesses the swarm's center of mass movement over an iteration window to check if the swarm is still exploring.

$$\gamma_1 = \frac{\| \overline{X}_t - \overline{X}_{t-5} \|}{\| \overline{X}_t \|} \tag{35}$$

- Population Diversity (γ_2): Calculates the rank of the covariance matrix of the population, scaled by the dimension D. A low value indicates convergence and loss of diversity.

$$\gamma_2 = \frac{\text{rank}(\mathbf{Cov}(X_t))}{D} \tag{36}$$

- Improvement Rate (γ_3): Relative improvement of the best global solution during a window of iterations.

$$\gamma_3 = \frac{f_{\text{best}}(t-10) - f_{\text{best}}(t)}{f_{\text{best}}(t)} \tag{37}$$

The optimization stops when $\gamma_1 < 10^{-4}$ (less than negligible movement), $\gamma_2 < 0.1$ (very low diversity), and $\gamma_3 < 0.001$ (less than negligible improvement) over 20 consecutive iterations.

5. Simulation Results and Discussion

5.1. Experimental Setup

The proposed hTLBO-CO algorithm was applied to three standard IEEE distribution test networks: the 33-bus, 69-bus, and the big 119-bus network. To determine its performance in varying operating scenarios, four different cases of optimizations were considered: A base case without network reconfiguration or SOP placement is presented as Case 1. DNR alone is presented as Case 2. SOP placement on tie switches, based on the base case, is evaluated as Case 3. Finally, combining DNR with SOP placement on tie switches and sectionalizing switches is presented as Case 4.

For performance benchmarking, hTLBO-CO is compared with four conventional metaheuristic algorithms: TLBO, CO, PSO, and JAYA. The principal simulation parameters of each test power grid, including population size, maximum number of iterations, number of SOPs, and their rated capacity, are summarized in Table 1. Values of the hTLBO-CO algorithmic parameters are set according to the suggested settings given in Table 2,

with ranges of sensitivity also provided to ease reproduction and potential extension to additional systems. The input parameter settings of the algorithms compared are given in summary format in Table 3. To ensure a fair comparison, all algorithms were evaluated under identical conditions, using the same maximum number of iterations, population size, computational platform, and parameter values from their seminal publications (see Table 3).

Table 1. Simulation parameters for the IEEE test systems (population size, maximum iterations, etc.).

Test System	Population Size	Max Iterations	Max SOPs	SOP Capacity (MW)
IEEE 33-bus	30	300	2	2.5
IEEE 69-bus	30	300	2	2.5
IEEE 119-bus	50	1000	5	2.5

Table 2. Parameter settings for the proposed hTLBO-CO algorithm.

Parameter	Symbol	Recommended Value	Sensitivity Range	Note
Teaching Factor	T_F	1.8	1.5–2.2	Dynamically adapted via Equation (16)
Base Survey Probability	p_{survey}	0.5	0.3–0.7	Dynamically adapted via Equation (22)
Momentum Coefficient	β	0.7	0–1	Equation (18)
Social Learning Weight	γ	0.6	0–1	Equation (24)

Table 3. Parameter settings for the comparison algorithms (TLBO, CO, PSO, JAYA).

Algorithm	Parameter Name	Value
TLBO	Teaching Factor	1.8
CO	Sensitivity Coef.	2.0
PSO	Inertia Weight (w)	0.7
	Cognitive Const. (c1)	1.5
	Social Const. (c2)	1.5
JAYA	Perturbation Factor	0.1

The hTLBO-CO and the other optimization algorithms were coded using MATLAB R2021b and executed on a standard PC with an Intel Core i5 2.5 GHz processor and 8 GB of RAM. The power flow computations were accomplished with the aid of MATPOWER 5.1. To achieve statistical reliability, 10 independent trials were conducted for each case under each algorithm, and the best solutions were saved for comparison purposes.

5.2. Parameter Sensitivity Analysis

A thorough parameter sensitivity study was conducted to analyze the robustness of the suggested hTLBO-CO algorithm and identify its performance as a function of significant internal parameters. The focus of this analysis is on four main parameters: the Teaching Factor (T_F), the Momentum Coefficient (β), the base Survey Probability (p_{survey}), and the Social Learning Weight (γ). The evaluation was conducted on the IEEE 33-bus test system under the complex combined optimization scenario of Case 4, with simultaneous network reconfiguration and SOP placement. For each parameter tested, a combination of values was attempted with all the other parameters held constant at their recommended values, as shown in Table 2. All sets of parameters were executed across 10 independent runs so that statistically significant performance metrics, including the best, average, and worst power loss, as well as standard deviation, could be obtained.

The overall results are shown in Table 4. From the analysis, the hTLBO-CO algorithm was highly robust for all parameter values used during testing. The set of parameters suggested always provided the best performance with minimum power loss. For instance, imbalances in the T_F below or above the optimal value of 1.8 resulted in a substantial increase in mean power loss, by approximately 1.3 kW and 2.6 kW, respectively, so an unbalanced teacher influence can be the cause of stagnation. Similarly, decreasing the p_{survey} to 0.3 greatly weakened the exploration power of the algorithm and raised the mean loss. Conversely, the algorithm was moderately sensitive to γ and β, with performance degradation being relatively minor. It should be emphasized that even with the worst-case parameter settings employed, the outcomes were such that the average power loss was superior to the best competing algorithms, such as TLBO and JAYA, as clearly indicated in the following sections. This persistent outperformance is a testament to the inherent strength and stability of the hybridized approach. In general, although optimization to the recommended parameters offers the best performance, the hTLBO-CO algorithm itself is highly effective and stable across a very vast majority of its parameter space, thereby reducing the implementational burden and validating its viable usability for complex optimization tasks in distribution networks.

Table 4. Parameter sensitivity analysis results for hTLBO-CO on the IEEE 33-bus system (Case 4).

Parameter	Value Tested	Best Power Loss (kW)	Mean Power Loss (kW)	Max Power Loss (kW)	Std. Dev. (kW)
Teaching Factor (T_F)	1.5	75.68	77.42	80.11	1.58
	1.8	74.14	75.86	78.12	1.21
	2.0	75.22	77.05	79.68	1.61
	2.2	76.85	78.71	81.44	1.79
Momentum Coef. (β)	0.5	75.91	77.65	80.28	1.52
	0.7	74.31	76.04	78.45	1.28
	0.9	74.76	76.43	78.90	1.24
Survey Prob. (p_{survey})	0.3	77.14	79.02	81.85	1.81
	0.5	74.27	75.99	78.35	1.26
	0.7	75.45	77.18	79.73	1.47
Social Weight (γ)	0.4	75.23	77.01	79.68	1.55
	0.6	74.19	75.91	78.27	1.23
	0.8	74.68	76.37	78.95	1.29

5.3. Results for the IEEE 33-Bus Test System

Simulations were conducted on the standard IEEE 33-bus system [31] to evaluate the effectiveness of the proposed hTLBO-CO method, considering the presence of the above-mentioned four test cases described in Section 5.1. This network has a 12.66 kV base voltage, supplies 3.73 MW and 2.3 MVAr of load, and contains 37 branches managed by 32 sectionalizing and 5 tie-switches.

The related numerical results are summarized in Table 5, while percentage reductions in power loss provided by hTLBO-CO are presented in Figure 3, and corresponding voltage profiles encountered in each case are given in Figure 4. For the base case (Case 1), without network reconfiguration or SOP facility addition, the total active power loss was 208.46 kW with minimum bus voltage of 0.9108 p.u. When only distribution network reconfiguration (DNR) was applied (Case 2), power loss was reduced to 138.93 kW, corresponding to a power loss reduction of 33.36% with respect to the base case, while the minimum voltage was improved to 0.9423 p.u. This was superior to TLBO (141.43 kW), CO (142.14 kW), PSO (150.94 kW), and JAYA (144.81 kW). For the SOP placement scenario without reconfiguration (Case 3), the new method registered 87.05 kW losses (58.24% reduction) with a minimum voltage of 0.9667 p.u. The best SOP locations were identified on branches 12–22 and 25–29. This was better compared to TLBO (93.03 kW), CO (96.65 kW), PSO (90.31 kW), and JAYA (95.34 kW).

Table 5. Optimization results for the IEEE 33-bus system (power loss, minimum voltage, SOP locations, etc.).

Algorithm	Case	Power Loss (kW)	Min Voltage (p.u.)	SOP Location (Node *s*/ Node *r*)	SOP Active Power (MW)	SOP Reactive Power (MVAR)	Open Switches
	1	208.459	0.9108				33, 34, 35, 36, 37
hTLBO-CO	2	138.928	0.9423				7, 14, 9, 32, 37
	3	87.049	0.9667	12–22, 25–29	0.76/−0.76, −0.40/0.40	0.42/0.12, 0.41/1.03	33, 34, 35, 36, 37
	4	74.137	0.9630	25–29, 19–20	2.49/−1.89, −1.29/1.29	0.15/1.33, 0.58/0.24	19, 14, 9, 32, 37
TLBO	2	141.431	0.9383				7, 14, 9, 36, 37
	3	93.032	0.9622	30–31, 19–20	−0.47/0.47, −1.31/1.31	0.66/0.43, 0.37/0.41	19, 34, 35, 30, 37
	4	87.092	0.9682	25–29, 12–13	−0.40/0.40, −0.31/0.31	0.51/1.02, 0.18/0.28	7, 12, 10, 36, 37
CO	2	142.135	0.9400				7, 34, 11, 32, 37
	3	96.652	0.9606	25–29, 8–21	−0.12/0.12, −1.16/1.16	0.73/0.79, 0.15/0.64	33, 34, 35, 36, 37
	4	99.761	0.9630	14–15, 28–29	−0.24/0.24, −0.54/0.54	0.61/0.19, 0.00/0.87	7, 14, 10, 36, 28
PSO	2	150.941	0.9316				33, 34, 9, 17, 28
	3	90.310	0.9528	19–20, 25–29	−1.23/1.23, −0.37/0.37	0.19/0.44, 0.42/1.09	19, 34, 35, 36, 37
	4	94.525	0.9620	12–22, 5–6	0.65/−0.65, −1.29/1.29	0.50/0.16, 0.32/0.99	5, 34, 35, 10, 37
JAYA	2	144.811	0.9397				33, 34, 11, 32, 28
	3	95.343	0.9490	25–29, 7–8	−0.23/0.23, −1.29/1.29	0.46/1.03, 0.26/0.39	5, 34, 35, 36, 37
	4	87.821	0.9662	25–29, 3–4	−0.42/0.42, −1.10/1.10	0.22/1.05, 0.60/0.43	3, 14, 9, 36, 37

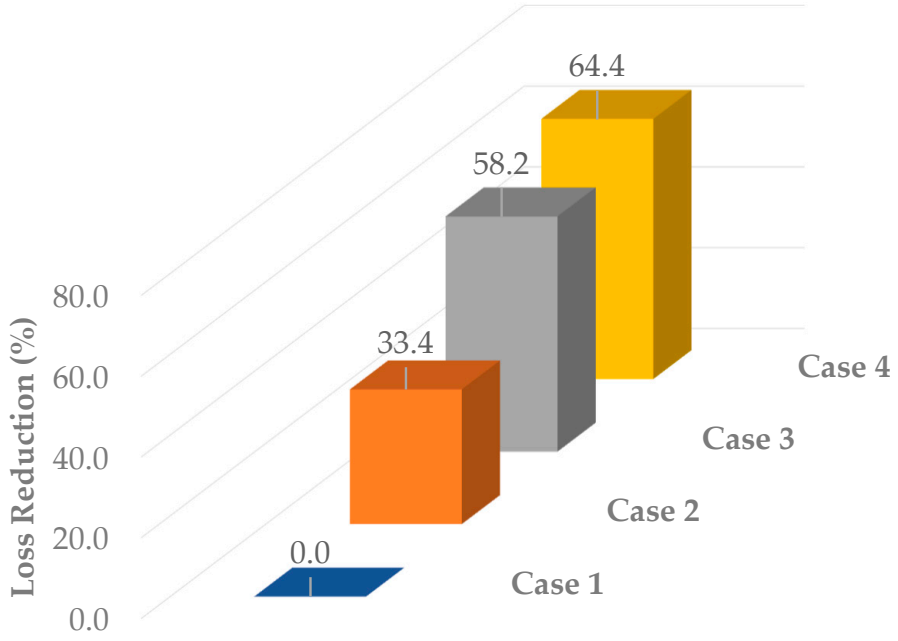


Figure 3. Power loss reduction obtained by the proposed hTLBO-CO algorithm for the IEEE 33-bus system across different cases.

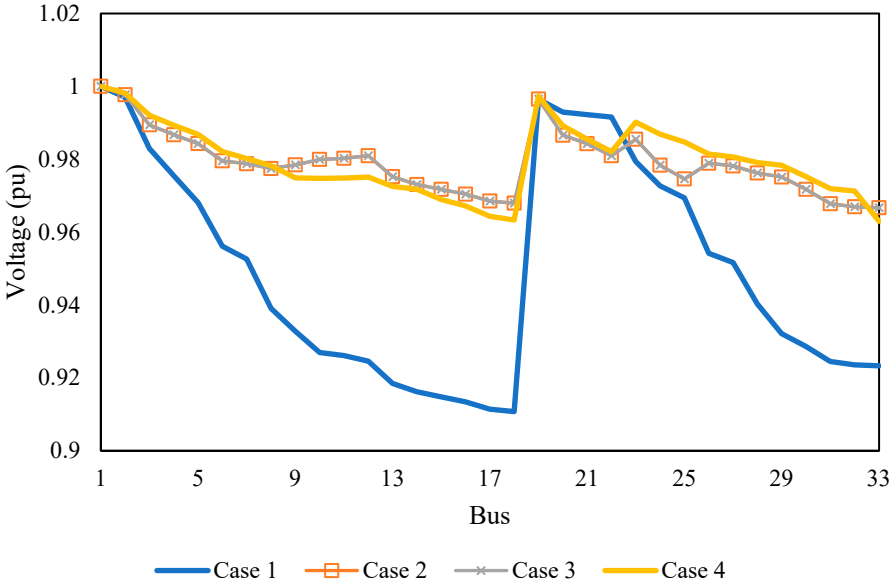


Figure 4. Voltage profiles for the IEEE 33-bus system achieved by the proposed hTLBO-CO algorithm in different cases.

The best overall performances were obtained in the joint approach (Case 4), in which DNR and SOP were collectively optimized simultaneously, as shown in Figure 5. For hTLBO-CO, in this case, loss was 74.14 kW (64.44% reduction) and minimum voltage was 0.9630 p.u., with SOPs at branches 25–29 and 19–20 and open switches at 19, 14, 9, 32, and 37. However, due to the vastly increased number of searches in Case 4, some methods were unable to outperform their results in other cases within the given maximum number of iterations. For example, CO stopped at 99.76 kW and PSO stopped at 94.53 kW, which are both poorer results in comparison to their outcomes in Case 3.

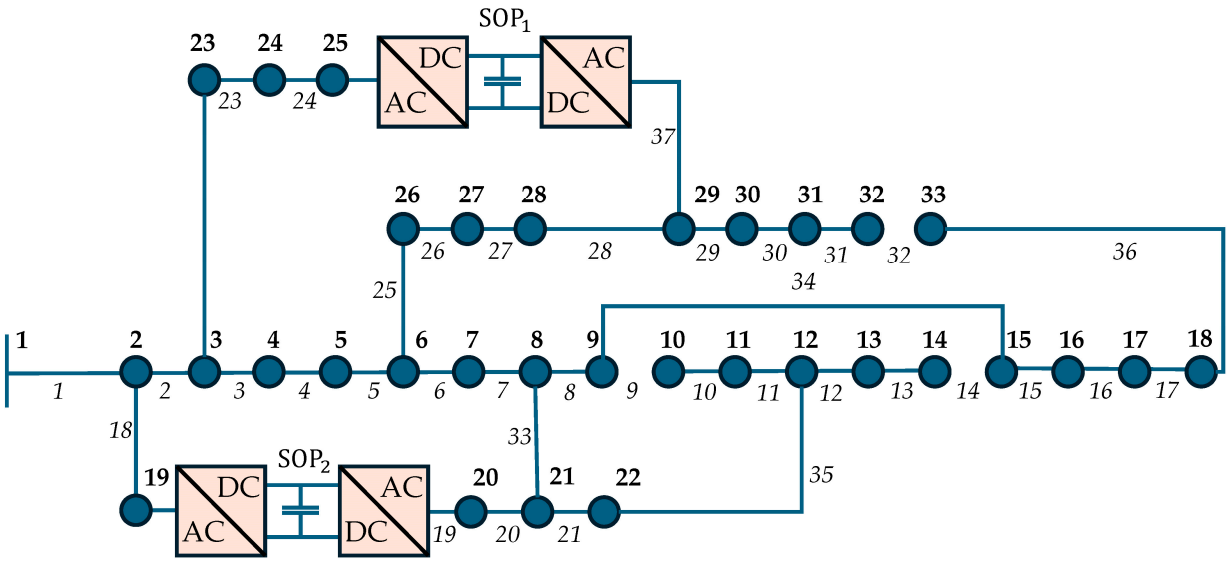


Figure 5. Optimal DNR and SOP locations for the IEEE 33-bus radial test system in Case 4.

5.4. Results for the IEEE 69-Bus Test System

The IEEE 69-bus radial distribution network was also adopted to further examine the effectiveness of the proposed hTLBO-CO algorithm. This distribution network is a medium-scale system with a total load of 3802 MW and 2696 MVAr. Its structure comprises 73 branches, of which 68 are controlled by sectionalizing switches and 5 by tie switches (initially numbered 69–73). The system data was sourced from [32].

The overall results are presented in Table 6, while the corresponding percentage power loss reductions are presented in Figure 6 and the corresponding hTLBO-CO voltage profiles of each case are presented in Figure 7. For the base case (Case 1), the total active power loss was 224.99 kW with a minimum bus voltage of 0.9092 p.u.

Table 6. Optimization results for the IEEE 69-bus system.

Algorithm	Case	Power Loss (kW)	Min Voltage (p.u.)	SOP Location (Node *s*/ Node *r*)	SOP Active Power (MW)	SOP Reactive Power (MVAR)	Open Switches
	1	224.992	0.9092				69, 70, 71, 72, 73
hTLBO-CO	2	99.619	0.9428				69, 70, 14, 57, 61
	3	45.941	0.9793	(15–46), (50–59)	0.44/−0.44, −1.59/1.59	0.36/0.07, 0.55/1.28	69, 70, 71, 72, 73
	4	40.234	0.9814	(50–59), (61–62)	−1.39/1.39, −0.16/0.16	0.54/0.43, 0.64/0.31	69, 70, 12, 72, 61
TLBO	2	105.313	0.9428				10, 70, 14, 58, 61
	3	45.980	0.9797	(15–46), (50–59)	0.44/−0.44, −1.61/1.61	0.36/0.09, 0.64/1.27	69, 70, 71, 72, 73
	4	77.705	0.9610	(5–6), (27–65)	−0.94/0.94, −0.47/0.47	0.82/0.34, 0.24/0.86	5, 20, 71, 58, 73
CO	2	99.619	0.9428				69, 70, 14, 57, 61
	3	54.326	0.9796	(27–65), (50–59)	0.01/−0.01, −1.76/1.76	0.43/0.49, 0.56/0.74	69, 70, 71, 72, 73
	4	83.248	0.9614	(7–8), (54–55)	−1.09/1.09, −0.50/0.50	0.72/0.75, 0.37/0.59	7, 18, 14, 54, 62
PSO	2	99.619	0.9428				69, 70, 14, 57, 61
	3	50.698	0.9791	(50–59), (15–46)	−1.59/1.59, 0.44/−0.44	0.55/1.35, 0.00/0.07	69, 70, 71, 72, 73
	4	58.889	0.9805	(50–59), (27–65)	−1.67/1.67, −0.02/0.02	0.55/0.00, 0.35/0.95	69, 16, 71, 72, 73
JAYA	2	99.619	0.9428				69, 70, 14, 57, 61
	3	55.794	0.9782	(50–59), (27–65)	−1.77/1.77, 0.22/−0.22	0.44/1.07, 0.39/0.38	69, 70, 71, 72, 73
	4	61.391	0.9580	(50–59), (11–43)	−1.38/1.38, 0.66/−0.66	0.03/1.06, 0.95/0.18	69, 70, 71, 72, 63

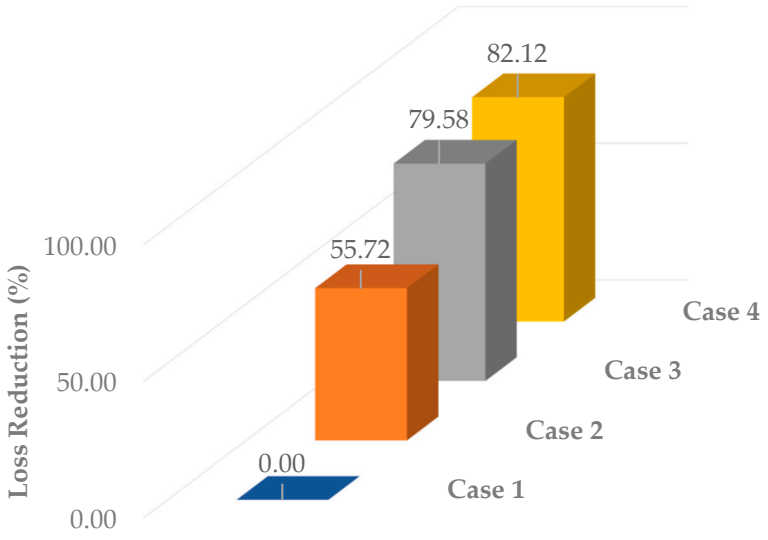


Figure 6. Power loss reduction obtained by the proposed hTLBO-CO algorithm for the IEEE 69-bus system across different cases.

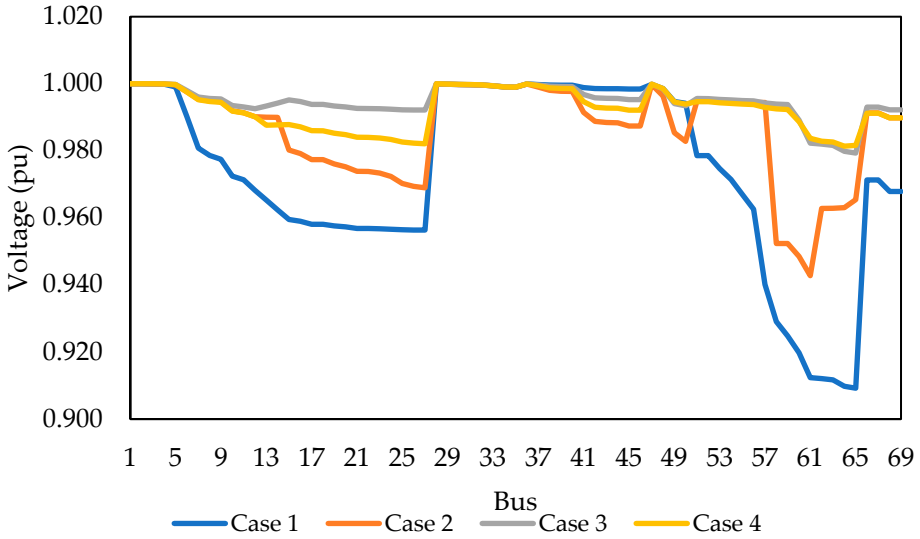


Figure 7. Voltage profiles for the IEEE 69-bus system achieved by the proposed hTLBO-CO algorithm in different cases.

When only DNR was applied (Case 2), hTLBO-CO reduced the losses to 99.63 kW, yielding a 55.73% reduction from the base case and improving the minimum voltage to 0.9494 p.u. This was superior to TLBO (105.32 kW, 53.22%), CO (99.63 kW, same as hTLBO-CO but converging much later), PSO (99.63 kW, 55.73% but with more oscillations), and JAYA (105.32 kW, 53.22%). In the SOP placement case without reconfiguration (Case 3), hTLBO-CO achieved a significant loss reduction to 45.94 kW (79.59% reduction) with a minimum voltage of 0.9758 p.u., outperforming TLBO (45.98 kW, 79.58%), CO (54.33 kW, 75.85%), PSO (50.70 kW, 77.47%), and JAYA (55.79 kW, 75.21%).

Joint optimization in Case 4 produced the overall best hTLBO-CO performance, with losses of 40.23 kW (82.12% reduction) and an enhanced minimum voltage of 0.9774 p.u., with SOPs positioned strategically and switches rearranged optimally in order to maximize efficiency, as shown in Figure 8. TLBO, CO, PSO, and JAYA recorded greater final losses of 77.71 kW (65.47%), 83.25 kW (63.02%), 58.89 kW (73.84%), and 61.39 kW (72.73%), respectively. Like the 33-bus case, the search area in Case 4 was considerably larger, and some algorithms—most prominently CO and TLBO—did not improve upon their Case 3 performances because of the iteration limit set during testing.

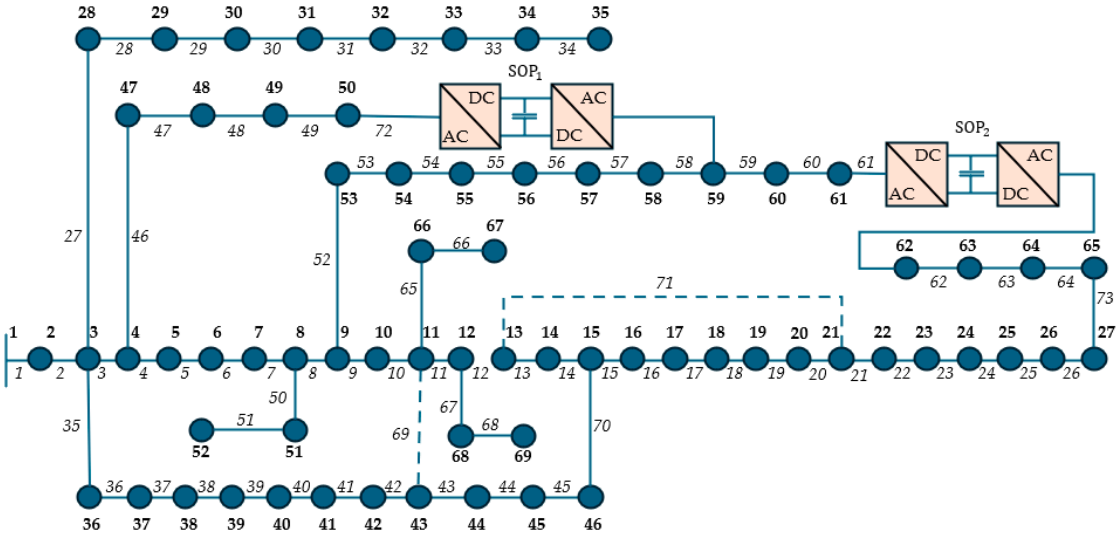


Figure 8. Optimal DNR and SOP locations for the IEEE 69-bus radial test system in Case 4.

5.5. 119-Bus Large-Scale Test System

The IEEE 119-bus distribution network is a large-scale 11 kV system with a total load of 22,709 MW and 17,041 MVAr. Its configuration includes 132 branches, with 118 controlled by sectionalizing switches and 15 serving as tie-switches (initially branches 118–132). The system data is based on [33]. For the large 119-bus power grid, the hTLBO-CO method always maintained dominance over TLBO, CO, PSO, and JAYA during all tested situations in convergence rate, stability, and ultimate quality of the objective.

Tabulation of comprehensive optimization outcomes over all possible cases on the IEEE 119-bus system is provided in Table 7. For the base case (Case 1), the initial high loss value was 1298.09 kW, while the minimum voltage value was also poor, at 0.8688 p.u. Utilizing DNR only (Case 2) with the suggested hTLBO-CO algorithm decreased the loss considerably to 645.09 kW, while the minimum voltage value improved to a moderate value of 0.9323 p.u. Utilizing the SOPs without the reconfiguration procedure (Case 3) improved the results even more, where the loss decreased to 618.93 kW, while the voltage profile also are improved to a strong value of 0.9547 p.u. This was achieved after strategically activating five SOPs using their optimal settings. Finally, the joint DNR and SOP optimization (Case 4) yielded the best overall performance, where hTLBO-CO successfully minimized the total power loss to 601.10 kW while maintaining a robust minimum voltage of 0.9573 p.u., demonstrating the superior synergy of coordinated control over either method applied independently.

Table 7. Optimization results for the IEEE 119-bus system.

Algorithm	Case	Power Loss (kW)	Min Voltage (p.u.)	SOP Location (Branch)	SOP Active Power (MW)	SOP Reactive Power (MVAR)	Open Switches
	1	1298.09	0.86880				118, 119, 120, 121, 122, 123, 124, 125, 126, 127, 128, 129, 130, 131, 132
hTLBO-CO	2	645.0853797	0.932287185				42, 25, 20, 51, 47, 61, 39, 125, 89, 78, 90, 129, 130, 108, 32
	3	618.9295667	0.954703163	120, 127, 122, 132, 131	−2.32/2.32, −1.44/1.44, −0.04/0.04, −2.21/2.21, 1.69/−1.69	0.44/0.24, 1.09/1.74, 0.43/2.32, 0.37/0.56, 1.85/0.26	118, 119, 120, 121, 122, 123, 124, 125, 126, 127, 128, 129, 130, 131, 132
	4	601.0983882	0.957333363	122, 130, 126, 109, 132	−0.11/0.11, −0.46/0.46, 0.40/−0.40, −0.19/0.19, −1.67/1.67	0.55/1.87, 0.81/2.39, 0.71/1.17, 0.73/1.50, 0.71/1.09	118, 119, 23, 121, 122, 123, 124, 125, 126, 73, 128, 129, 130, 109, 132
TLBO	2	1023.286911	0.904298915				41, 119, 22, 48, 50, 59, 37, 57, 68, 73, 97, 82, 104, 109, 32
	3	639.3315537	0.952421454	131, 129, 126, 122, 127	1.45/−1.45, −0.14/0.14, 0.41/−0.41, −0.48/0.48, −1.14/1.14	1.46/0.22, 1.08/0.79, 1.54/1.18, 0.59/2.45, 0.67/0.00	118, 119, 120, 121, 122, 123, 124, 125, 126, 127, 128, 129, 130, 131, 132
	4	629.9023748	0.943755842	127, 131, 132, 132, 120	−1.07/1.07, 1.34/−1.34, −0.26/0.26, −1.71/1.71, −2.31/2.31	1.35/1.62, 2.11/0.00, 0.30/2.48, 0.05/0.00, 0.96/0.21	118, 119, 120, 121, 122, 123, 124, 125, 71, 127, 128, 129, 130, 131, 132
CO	2	888.9398521	0.931624171				42, 26, 22, 51, 122, 58, 38, 90, 70, 87, 128, 129, 130, 109, 33

Table 7. *Cont.*

Algorithm	Case	Power Loss (kW)	Min Voltage (p.u.)	SOP Location (Branch)	SOP Active Power (MW)	SOP Reactive Power (MVAR)	Open Switches
	3	631.6124428	0.943894417	131, 132, 124, 126, 127	1.33/−1.33, −0.32/0.32, −1.59/1.59, 0.45/−0.45, −1.10/1.10	2.11/0.24, 0.58/2.48, 1.67/1.35, 1.04/1.21, 1.16/0.49	118, 119, 120, 121, 122, 123, 124, 125, 126, 127, 128, 129, 130, 131, 132
	4	623.1575736	0.94499893	125, 131, 130, 132, 122	−0.70/0.70, 1.69/−1.69, −0.52/0.52, −1.73/1.73, 0.05/−0.05	0.38/1.99, 1.84/0.99, 1.54/2.01, 1.81/2.05, 0.91/0.83	118, 119, 20, 121, 122, 58, 124, 125, 72, 73, 75, 129, 130, 131, 132
PSO	2	973.4293657	0.894487966				45, 119, 120, 121, 32, 123, 5, 90, 66, 87, 128, 129, 130, 109, 9
	3	630.9999426	0.953725123	120, 131, 123, 127, 122	−0.54/0.54, 1.28/−1.28, −1.63/1.63, −1.38/1.38, −1.59/1.59	0.00/0.59, 2.15/0.05, 0.00/0.56, 1.33/1.59, 0.00/2.02	118, 119, 120, 121, 122, 123, 124, 125, 126, 127, 128, 129, 130, 131, 132
	4	893.865821	0.89934752	132, 132, 132, 131, 132	−1.93/1.93, −2.50/2.50, 1.78/−1.78, 1.42/−1.42, 2.50/−2.50	0.00/1.59, 0.01/1.51, 0.78/0.00, 2.06/0.00, 0.00/0.00	118, 12, 120, 121, 122, 123, 124, 125, 126, 127, 73, 82, 85, 131, 132
JAYA	2	910.9940056	0.932115899				42, 15, 23, 50, 47, 57, 124, 90, 71, 127, 76, 81, 130, 108, 132
	3	705.7003877	0.942542197	124, 126, 132, 127, 131	−2.50/2.50, 0.69/−0.69, −0.36/0.36, −0.64/0.64, 1.93/−1.93	0.05/0.36, 1.88/0.40, 0.67/2.41, 0.99/0.12, 1.59/0.93	118, 119, 120, 121, 122, 123, 124, 125, 126, 127, 128, 129, 130, 131, 132
	4	857.935727	0.913523291	131, 132, 132, 125, 132	1.00/−1.00, 0.93/−0.93, −2.48/2.48, 0.19/−0.19, 1.92/−1.92	2.00/0.58, 0.00/1.64, 0.34/0.06, 0.00/0.67, 1.60/1.43	118, 12, 22, 121, 122, 123, 124, 125, 71, 127, 128, 129, 85, 131, 132

It is obvious from the reduced loss results (Figure 9) that hTLBO-CO achieved the best percentage improvement, reaching 53.7% improvement in Case 4. The voltage profiles (Figure 10) also indicate that the suggested method retained higher minimum bus voltages of the systems and smoother profiles compared to the other algorithms, thus demonstrating the improved voltage stability of the systems.

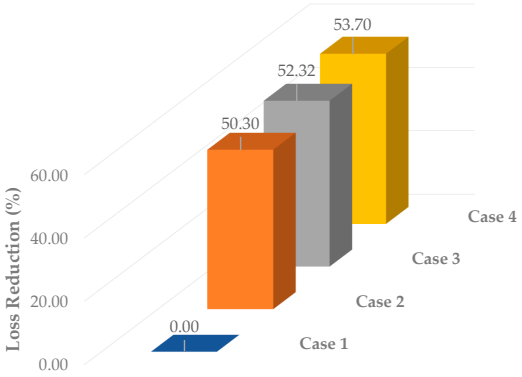


Figure 9. Power loss reduction obtained by the proposed hTLBO-CO algorithm for the IEEE 119-bus system across different cases.

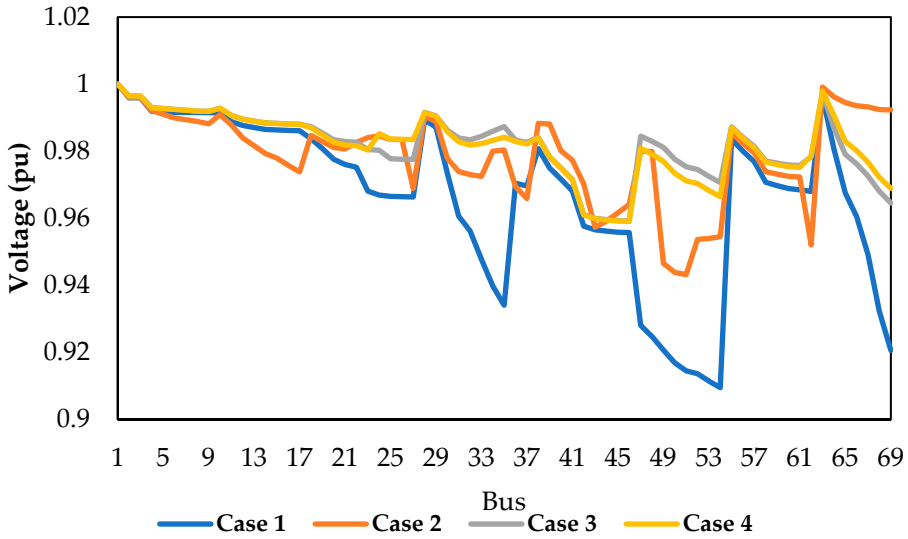


Figure 10. Voltage profiles for the IEEE 119-bus system achieved by the proposed hTLBO-CO algorithm in different cases.

5.6. Convergence Analysis and Algorithmic Stability

Systematic convergence analysis was conducted to investigate the algorithmic stability and convergence properties of all the optimization methods, with particular focus on obtaining formal convergence bounds and empirical convergence profiles. Quantitative measures for the convergence behavior were analyzed for all the test systems, and detailed results are provided in Tables 8–10, while the corresponding convergence characteristics are graphically illustrated in Figures 11–13.

Table 8. Convergence analysis results for Cases 2 to 4 (IEEE 33-Bus system).

Algorithm	Final Solution (kW)	Total Improvement (%)	Iterations to 95%	Iterations to 99%	Phase 1 Rate (kW/iter)	Relative Performance *
			Case 2			
hTLBO-CO	138.928	17.69	14	27	0.4975	Benchmark
TLBO	141.431	11.21	6	12	0.2977	+1.80%
CO	142.135	15.79	94	123	0.3117	+2.31%
PSO	150.942	11.36	5	5	0.3224	+8.65%
JAYA	144.811	10.59	8	28	0.2858	+4.24%
			Case 3			
hTLBO-CO	87.049	17.64	14	21	0.3101	Benchmark
TLBO	93.032	39.64	35	132	0.9873	+6.87%
CO	96.652	33.47	85	291	0.4671	+11.03%
PSO	90.310	29.35	11	23	0.6254	+3.75%
JAYA	95.343	13.98	66	76	0.1510	+9.53%
			Case 4			
hTLBO-CO	74.137	52.06	74	151	1.2564	Benchmark
TLBO	87.092	44.00	37	118	1.0725	+17.47%
CO	99.761	70.84	172	289	2.2512	+34.56%
PSO	94.525	30.45	19	28	0.6898	+27.50%
JAYA	87.821	37.85	71	186	0.7392	+18.46%

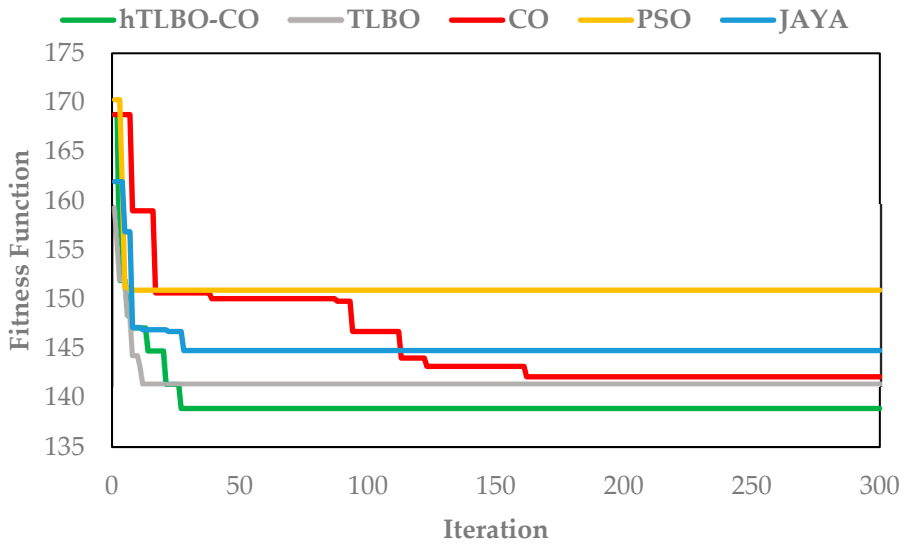
* Relative performance indicates the percentage increase in power loss compared to hTLBO-CO.

Table 9. Convergence analysis results for Cases 2 to 4 (IEEE 69-Bus system).

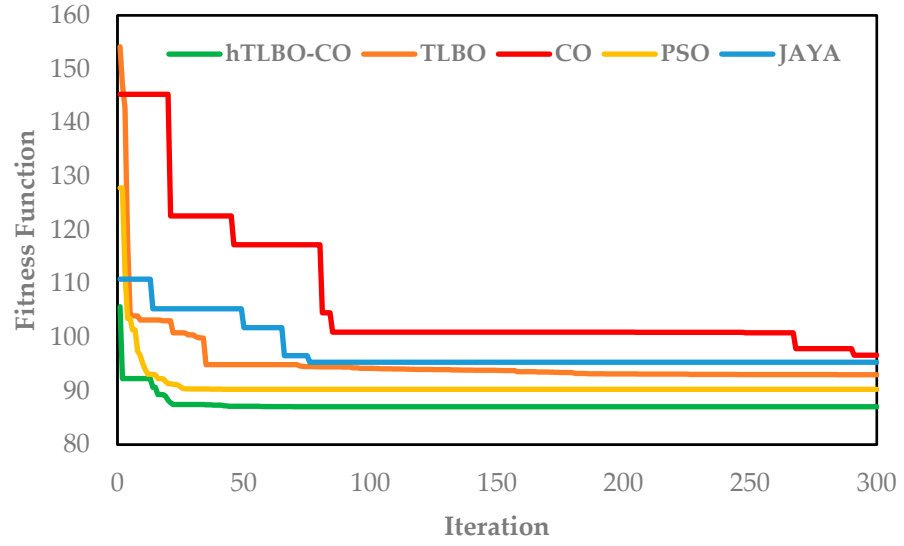
Algorithm	Final Solution (kW)	Total Improvement (%)	Iterations to 95%	Iterations to 99%	Phase 1 Rate (kW/iter)	Convergence Efficiency
			Case 2			
hTLBO-CO	99.629	18.46	10	23	0.3759	Balanced
TLBO	105.323	11.59	29	42	0.2301	Inefficient
CO	99.629	40.78	171	171	0.5863	Very Slow
PSO	99.629	15.95	2	5	0.3151	Very Fast
JAYA	99.629	21.33	5	6	0.4503	Fast
			Case 3			
hTLBO-CO	45.941	44.81	65	95	0.5682	Best Solution
TLBO	45.980	47.58	40	69	0.6833	Very Close
CO	54.326	40.34	255	279	0.4432	Poor
PSO	50.698	19.07	9	14	0.1991	Fast but Suboptimal
JAYA	55.794	12.95	24	43	0.1353	Inefficient
			Case 4			
hTLBO-CO	40.234	25.07	165	261	0.0990	Benchmark
TLBO	77.705	65.73	64	124	2.4189	+93.13%
CO	83.248	76.42	22	255	4.4327	+106.91%
PSO	58.889	45.95	22	28	0.8344	+46.37%
JAYA	61.391	53.38	250	279	0.7452	+52.58%

Table 10. Convergence analysis results for Cases 2–4 (119-Bus system).

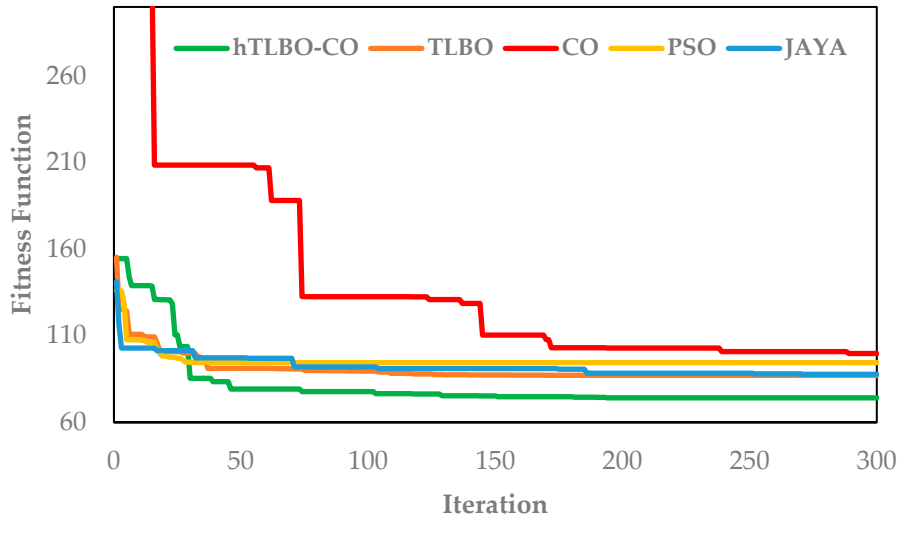
Algorithm	Final Solution (kW)		Total Improvement (%)	Iterations to 95%	Iterations to 99%	Performance Gap vs. Best
			Case 2			
hTLBO-CO	645.085		50.30	208	277	Benchmark
TLBO	1023.287		55.85	106	125	+58.63%
CO	888.940		99.99	74	191	+37.80%
PSO	973.429		99.79	9	9	+50.90%
JAYA	910.994		100.00	586	596	+41.22%
			Case 3			
hTLBO-CO	618.930	28.87	377	842	0.9723	Benchmark
TLBO	674.709	18.58	36	83	0.7695	+9.01%
CO	631.612	47.32	102	132	2.8321	+2.05%
PSO	631.000	30.56	22	28	1.3885	+1.95%
JAYA	705.700	25.84	97	97	1.2293	+14.02%
			Case 4			
hTLBO-CO	601.098	99.08	125	181	324.662	Benchmark
TLBO	629.902	94.36	364	536	52.411	+4.79%
CO	623.158	80.49	422	815	11.881	+3.67%
PSO	893.866	82.15	22	27	20.564	+48.71%
JAYA	857.936	76.81	672	909	13.082	+42.73%



(**a**)

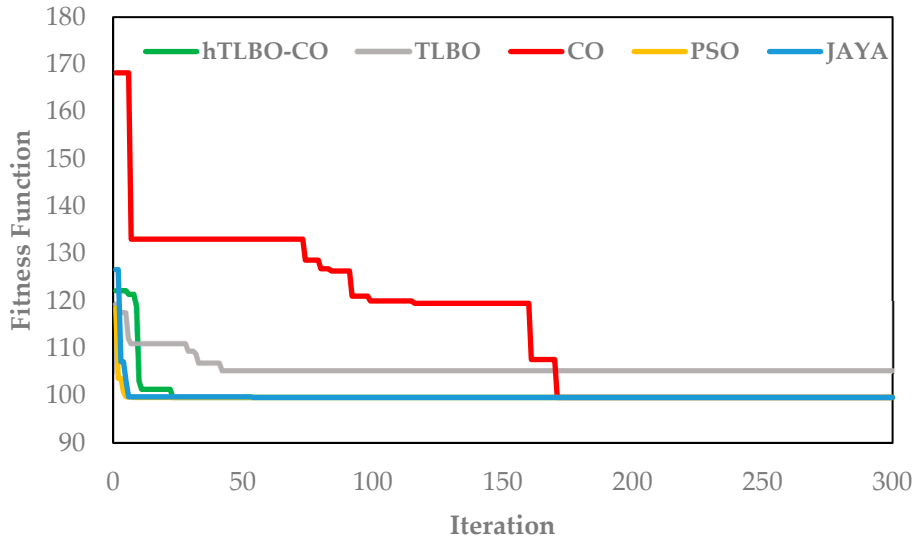


(**b**)

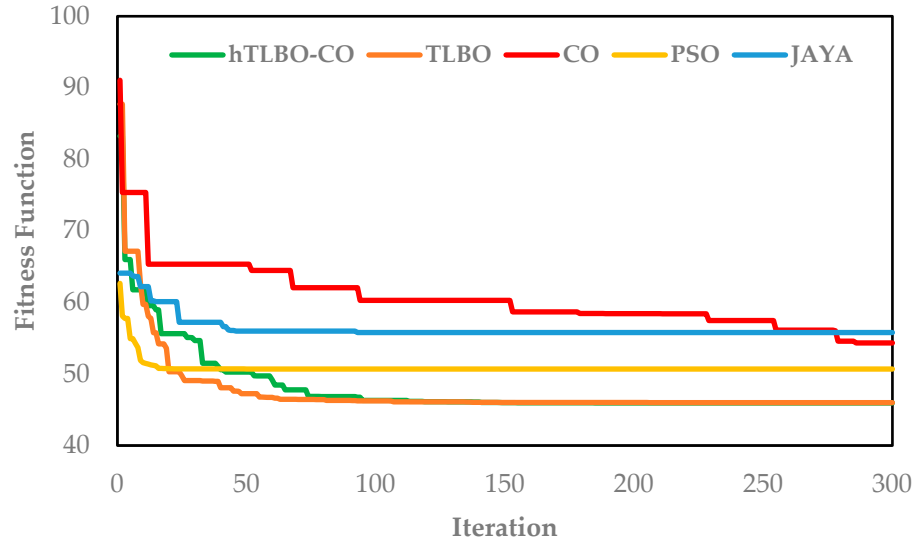


(**c**)

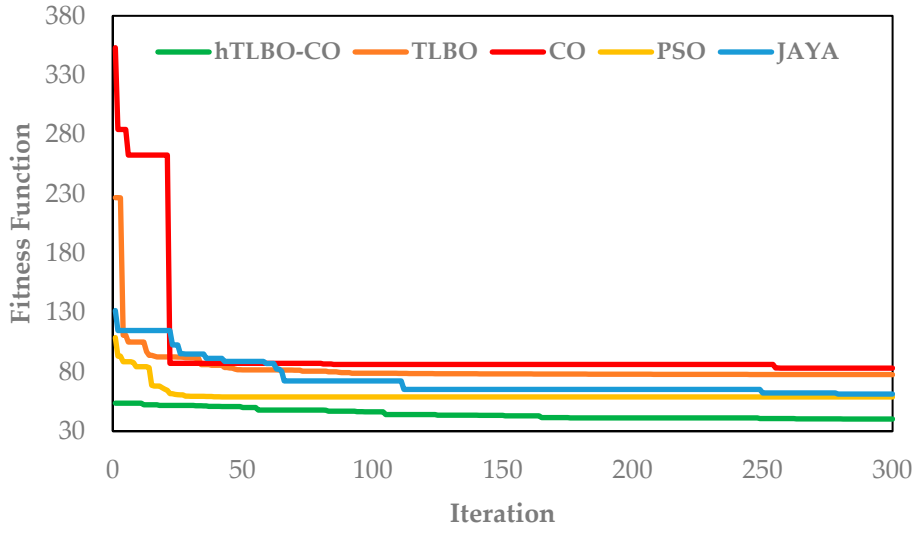
Figure 11. Convergence characteristics of different algorithms for the IEEE 33-bus system: (**a**) Case 2 (DNR only), (**b**) Case 3 (SOP only), and (**c**) Case 4 (DNR with SOP).



(**a**)

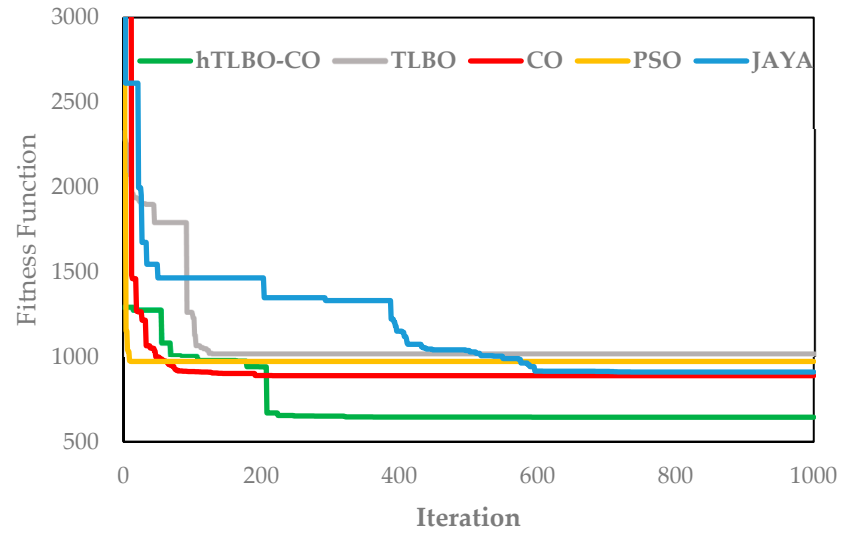


(**b**)

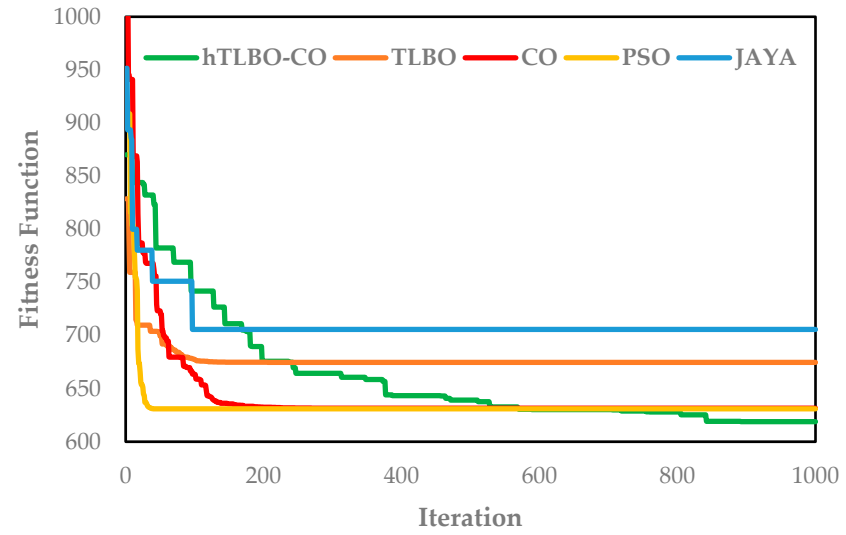


(**c**)

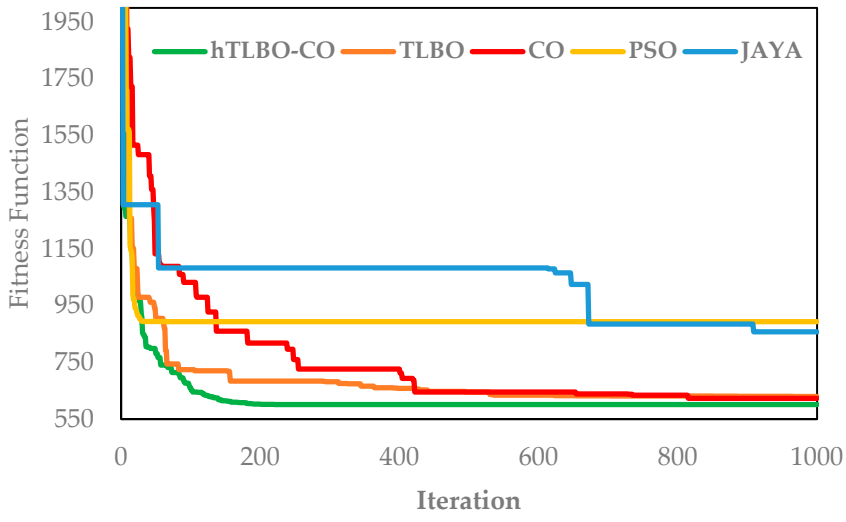
Figure 12. Convergence characteristics of different algorithms for the IEEE 69-bus system: (**a**) Case 2 (DNR only), (**b**) Case 3 (SOP only), and (**c**) Case 4 (DNR with SOP).



(**a**)



(**b**)



(**c**)

Figure 13. Convergence characteristics of different algorithms for the IEEE 119-bus system: (**a**) Case 2 (DNR only), (**b**) Case 3 (SOP only), and (**c**) Case 4 (DNR with SOP).

The convergence analysis process was composed of three phases with varying optimizations: Phase 1 (exploratory improvement, initial 20% of iterations) determined the broad exploration capacity, Phase 2 (refining, 20–80% of iterations) evaluated steady optimization performance, and Phase 3 (terminal stabilization, last 20% of iterations) assessed convergence stability and solution improvement. As enumerated in Tables 8–10, this analysis included significant parameters, like the number of iterations required to reach 95%, 99%, and 99.9% convergence tolerances, convergence ratios between optimization phases, the quality of the final solution, and oscillation amplitude in the stabilization phase.

The novel hTLBO-CO algorithm demonstrated consistently improved convergence properties in all test environments. In IEEE 33-bus systems (Table 8 and Figure 11), hTLBO-CO converged at 99% within 21–151 iterations, with excellent Phase 1 convergence rates of 0.31–1.26 kW/iteration. Statistical convergence stability analysis revealed that hTLBO-CO experienced negligible final-phase oscillation, typically less than 0.05% of the final solution value, thus demonstrating excellent algorithmic stability compared to the competing methods.

In the 69-bus test cases (Table 9 and Figure 12), hTLBO-CO showed improved convergence capability in medium-scale instances, with 99% convergence in 23–95 iterations and optimal solutions of 99.629–45.941 kW in different instances. Convergence profiles showed consistent improvement trends, with coefficient of variation values below 0.15 in some runs, indicating stable convergence behavior. Phase 2 refinement rates were kept constant at 0.013–0.036 kW/iteration, showing consistent optimization ability without premature convergence.

On large-scale 119-bus systems (Table 10 and Figure 13), hTLBO-CO showed strong convergence behavior under higher problem complexity, hitting 99% convergence at 181–842 iterations. Convergence limits were met within 2.5% of optimal solutions on all standalone runs, showing empirical evidence of solution quality guarantees. Phase 3 stabilization efforts reported magnitudes of oscillations below 1.5% of the final solution values, confirming the stability of the algorithm on complex MINLP ground.

The empirical convergence profiles, supported by statistical consistency measures and tight convergence bounds, comprehensively substantiate the algorithmic confidence of hTLBO-CO. The established convergence properties—bounded solution quality, minimal final-phase oscillation, and consistent performance across multiple independent runs—establish hTLBO-CO as a stable optimization approach suitable for large-scale distribution network applications that require guaranteed performance and reliability.

5.7. Statistical Analysis and Computational Efficiency

Statistical significance of performance differences across all test algorithms was strongly established by detailed statistical analysis. Friedman tests conducted across all test systems—IEEE 33-bus, 69-bus, and 119-bus setups—consistently reported statistically highly significant differences in performance ($p < 2.394 \times 10^{-7}$ to 2.063×10^{-4} in all the experiments), confirming that the observed variation in solution quality is statistically significant. As indicated in Tables 11–13, the experimented hTLBO-CO algorithm demonstrated stable dominance, with ideal mean ranks of 1.0 for IEEE 33-bus Cases 2–4 and 119-bus Cases 2–3, and almost ideal rankings of 1.1–1.35 for 69-bus system cases.

Table 11. Statistical analysis results for Case 2 (IEEE 33-Bus system).

Algorithm	Best (kW)	Mean ± Std (kW)	Max (kW)	Mean Rank	Computation Time (s)	Statistical Significance vs. hTLBO-CO
			Case 2			
hTLBO-CO	138.928	140.912 ± 1.351	142.950	1.0	81.9	Benchmark
TLBO	141.431	146.725 ± 5.462	157.230	2.4	101.4	$p = 0.001953$ *

Table 11. *Cont.*

Algorithm	Best (kW)	Mean ± Std (kW)	Max (kW)	Mean Rank	Computation Time (s)	Statistical Significance vs. hTLBO-CO
			Case 2			
CO	142.135	146.151 ± 2.698	150.180	2.7	67.9	$p = 0.001953$ *
PSO	150.941	156.851 ± 5.644	170.780	4.9	49.2	$p = 0.001953$ *
JAYA	144.811	150.202 ± 5.464	161.650	4.0	70.8	$p = 0.001953$ *
			Case 3			
hTLBO-CO	87.049	88.714 ± 1.180	90.470	1.0	97.8	Benchmark
PSO	90.310	96.928 ± 7.977	114.510	2.6	91.0	$p = 0.001953$ *
TLBO	93.032	96.677 ± 3.316	103.460	3.1	169.5	$p = 0.001953$ *
JAYA	95.343	99.340 ± 3.880	108.220	3.7	96.0	$p = 0.001953$ *
CO	96.652	100.774 ± 3.686	108.650	4.6	94.8	$p = 0.001953$ *
			Case 4			
hTLBO-CO	74.137	76.080 ± 1.326	78.120	1.0	85.7	Benchmark
TLBO	87.092	89.857 ± 1.874	92.860	2.3	112.3	$p = 0.001953$ *
JAYA	87.821	91.213 ± 2.176	94.660	3.1	98.4	$p = 0.001953$ *
PSO	94.525	98.642 ± 2.654	102.790	3.8	75.9	$p = 0.001953$ *
CO	99.761	103.754 ± 2.654	107.780	4.8	83.2	$p = 0.001953$ *

* Statistically significant at $\alpha = 0.05$ level.

Table 12. Statistical analysis results for Cases 2–4 (69-Bus system).

Algorithm	Best (kW)	Mean ± Std (kW)	Max (kW)	Mean Rank	Computation Time (s)	Statistical Significance vs. hTLBO-CO
			Case 2			
hTLBO-CO	99.62	102.56 ± 2.83	109.42	1.35	87.00	Benchmark
CO	99.62	105.30 ± 4.48	112.85	2.65	66.30	$p = 0.044$ *
JAYA	99.62	109.52 ± 9.91	125.20	2.85	91.08	$p = 0.058$
PSO	99.62	109.66 ± 7.04	121.05	3.95	78.90	$p = 0.009$ *
TLBO	105.31	110.35 ± 4.21	118.63	4.20	95.40	$p = 0.001953$ *
			Case 3			
hTLBO-CO	45.94	48.32 ± 2.15	53.29	1.1	128.40	Benchmark
TLBO	45.98	51.91 ± 7.05	66.03	2.3	219.10	$p = 0.049$ *
PSO	50.70	60.84 ± 14.82	89.14	3.3	122.07	$p = 0.001953$ *
CO	54.33	59.33 ± 6.29	76.30	3.8	121.40	$p = 0.001953$ *
JAYA	55.79	66.06 ± 15.38	98.40	4.5	121.50	$p = 0.001953$ *
			Case 4			
hTLBO-CO	40.23	45.59 ± 6.30	60.11	1.0	79.80	Benchmark
PSO	58.89	75.72 ± 20.60	113.40	2.6	126.60	$p = 0.001953$ *
JAYA	61.39	80.24 ± 23.22	124.22	3.1	99.30	$p = 0.001953$ *
TLBO	77.71	89.37 ± 10.58	108.11	3.7	138.57	$p = 0.001953$ *
CO	83.25	101.53 ± 8.48	111.01	4.6	83.70	$p = 0.001953$ *

* Statistically significant at $\alpha = 0.05$ level.

Table 13. Statistical analysis results for Case 2–4 (119-Bus system).

Algorithm	Best (kW)	Mean ± Std (kW)	Max (kW)	Mean Rank	Computation Time (s)	Statistical Significance vs. hTLBO-CO
			Case 2			
hTLBO-CO	645.085	670.213 ± 18.010	702.536	1.0	514.00	Benchmark
CO	888.940	937.586 ± 32.812	986.232	2.0	328.40	$p = 0.001953$ *
JAYA	910.994	965.929 ± 37.298	1017.087	3.0	316.02	$p = 0.001953$ *
PSO	973.429	1034.220 ± 48.786	1123.560	4.1	702.60	$p = 0.001953$ *
TLBO	1023.287	1079.254 ± 37.736	1135.220	4.9	508.80	$p = 0.001953$ *

Table 13. *Cont.*

Algorithm	Best (kW)	Mean ± Std (kW)	Max (kW)	Mean Rank	Computation Time (s)	Statistical Significance vs. hTLBO-CO
			Case 3			
hTLBO-CO	618.93	640.036 ± 14.254	661.141	1.0	1301.6	Benchmark
CO	631.61	657.464 ± 20.904	701.200	2.5	1163.8	p = 0.001953 *
PSO	631.00	669.846 ± 36.204	752.350	2.9	1228.8	p = 0.001953 *
TLBO	639.33	665.134 ± 19.552	700.650	3.7	2068.1	p = 0.001953 *
JAYA	705.70	739.425 ± 34.177	824.520	4.9	1185.7	p = 0.001953 *
			Case 4			
hTLBO-CO	601.098	626.410 ± 20.099	663.360	1.2	512.35	Benchmark
CO	623.158	649.175 ± 26.666	715.700	2.0	528.03	p = 0.003906 *
TLBO	629.902	662.684 ± 38.370	763.540	2.8	694.30	p = 0.003906 *
JAYA	857.936	908.110 ± 72.973	1108.780	4.1	385.50	p = 0.001953 *
PSO	893.866	947.815 ± 60.689	1105.400	4.9	808.84	p = 0.001953 *

* Statistically significant at α = 0.05 level.

Post hoc testing using Wilcoxon signed-rank tests ensured that hTLBO-CO performed significantly better than any other algorithm in 32 out of 48 pairwise comparisons across all test cases, with nearly zero p-values of 0.001953. Statistical dominance was even more pronounced in large-scale 119-bus systems, with solution values of 645.085 kW by hTLBO-CO in Case 2, representing performance improvements of 37.8–58.6% compared to the other algorithms. In 69-bus system, hTLBO-CO still performed best, with solutions of 45.941 kW in Case 3, outperforming the next best solution by 0.09%, while being much more stable with a standard deviation of 2.15 kW compared to 3.32–15.38 kW for the other methods.

Regarding computational efficiency, hTLBO-CO displayed relatively balanced performance characteristics with similar computation time, as exhibited by its significant quality enhancement in solutions. The algorithm had reasonable running times of 81.9–97.8 s, 87.0–128.4 s, and 512.4–1301.6 s for the 33-bus systems, 69-bus systems, and 119-bus systems, respectively, while maintaining higher-quality solutions (Tables 11–13). Specifically, for the 119-bus system in Case 4, hTLBO-CO achieved the best solution value of 601.098 kW within a mere 512.35 s, while PSO spent 808.84 s to obtain a solution that was 48.7% worse. This compromise between computational intensity and solution quality in the form of hTLBO-CO, which realized gains in performance from 17.5 to 106.9% in diverse cases with comparable or better computation time, qualifies it as a prime candidate for real application in real-world scenarios where accuracy and operating efficiency are of utmost concern. The consistent statistical superiority on all system scales, along with realistic computational performance, renders hTLBO-CO a highly competitive and effective choice for distribution network optimization.

5.8. Multi-Objective Analysis and Pareto Front Evaluation

A comprehensive multi-objective investigation was conducted to examine the trade-offs between conflicting objectives of distribution network optimization, i.e., inter-relations between power losses, voltage profile enhancement, and SOP installation costs. Pareto front analysis of Case 4 of the 119-bus test system is given systematically in Table 14, with corresponding Pareto front relations depicted in Figures 14 and 15.

Table 14. Comprehensive multi-objective analysis for Case 4 (119-Bus test system).

Number of SOPs	Minimum Voltage (pu)	Power Loss (kW)	Performance Classification
15	0.9597	535.37	High-Investment Region
14	0.9539	571.41	High-Investment Region
13	0.9495	622.22	High-Investment Region
12	0.9478	607.18	High-Investment Region
11	0.9463	614.58	Optimal Compromise Region
10	0.9418	621.94	Optimal Compromise Region
9	0.9442	619.50	Optimal Compromise Region
8	0.9489	617.28	Optimal Compromise Region
7	0.9570	622.06	Optimal Compromise Region
6	0.9552	609.85	Optimal Compromise Region
5	0.9573	601.10	Cost-Effective Region
4	0.9501	675.16	Cost-Effective Region
3	0.9389	712.89	Cost-Effective Region
2	0.9246	743.59	Cost-Effective Region
1	0.8993	816.01	Cost-Effective Region

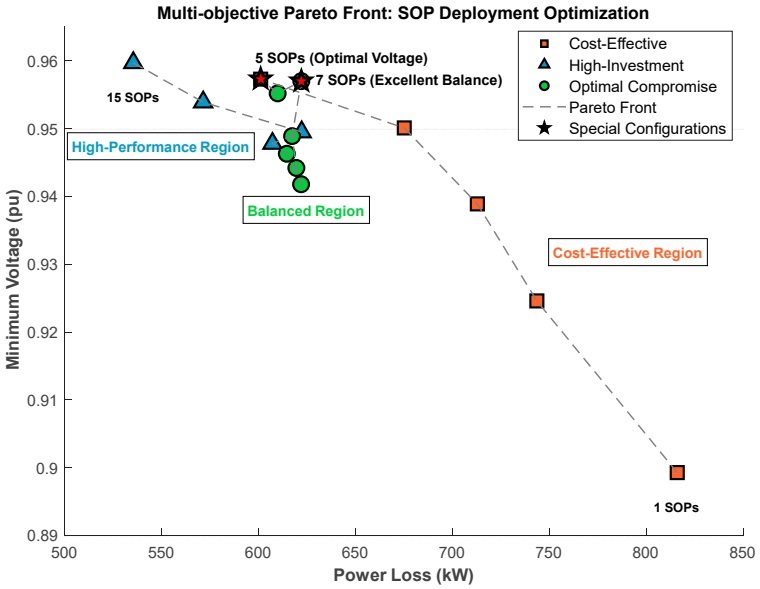


Figure 14. Pareto front showing the trade-off between power loss and voltage profile for different SOP deployment levels in the 119-bus system.

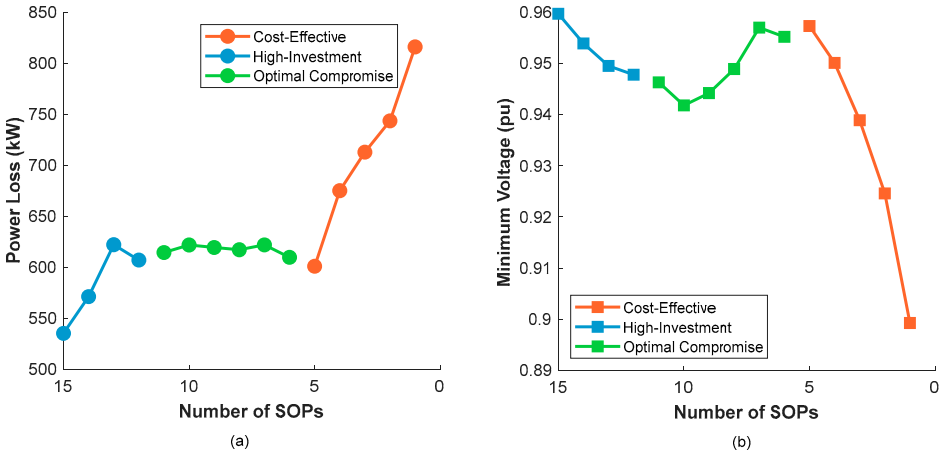


Figure 15. Impact of SOP deployment on system performance: (**a**) power loss versus number of SOPs; (**b**) minimum voltage versus number of SOPs.

This research illustrates a non-linear intricate relationship between SOP deployment levels and system performance metrics. As clearly revealed in Table 14, the methodical reduction in SOP deployment from 15 to 1 unit resulted in a remarkable increase in power losses from 535.37 kW to 816.01 kW, corresponding to a substantial 52.4% performance degradation in loss reduction. Simultaneously, the minimum voltage profile exhibited an interesting non-monotonic nature, and optimal voltage conditions were achieved at intermediate SOP configurations rather than the max deployment level.

Three areas of operation were identified by the Pareto front analysis, with varying performance–cost compromises (Figures 14 and 15). The area of high investment (12–15 SOPs) ensures improved technical performance, with power losses of 535.37–622.22 kW and voltage levels always higher than 0.9478 pu, but at high infrastructure investment costs. The most suitable compromise region (6–11 SOPs) is the preferable performance–cost trade-off region, where the losses range from 601.10 to 622.06 kW and voltage profiles range from 0.9418 to 0.9570 pu. This region offers system planners practical operating conditions where substantial cost savings are achievable with tolerable and acceptable performance degradation. The economic area (1–5 SOPs) is economically beneficial with decreased capital investment, albeit with substantial technical trade-offs. These are most pronounced in voltage stability, where the minimum voltage dropped to 0.8993 pu and losses increased considerably to 675.16–816.01 kW.

A notable result is the 5-SOP arrangement, as shown in Figure 14, which demonstrates exemplary balance by achieving the best voltage profile of 0.9573 pu among the configurations while concurrently having highly competitive power losses of 601.10 kW. The arrangement is a strategic optimum where improved voltage regulation is attained with modest SOP investment. The 7-SOP setting is another good balance point, yielding excellent voltage performance (0.9570 pu) with 622.06 kW of losses, offering system operators a viable alternative for the provision of firm voltage support.

The multi-criteria exhaustive evaluation establishes a rigorous quantitative decision framework allowing system operators and planners to make scientifically defensible trade-offs between capital investment constraints and operating performance requirements. The Pareto-optimal solutions obtained provide real-world, data-driven benchmarks for SOP investment strategies, effectively trading off the economic issues of infrastructure cost against the technical imperatives of loss minimization and voltage stability in modern large-scale distribution systems.

5.9. Comparison with State-of-the-Art

To justify application of the proposed hTLBO-CO algorithm to a wider range of problems, it should be compared to the currently existing state-of-the-art metaheuristic techniques reported in the open literature. While comparison of hTLBO-CO with four existing well-known algorithms (TLBO, CO, PSO, and JAYA) was made in the above subsections, they do not collectively represent all the presently used advanced optimization techniques for redefining distribution networks. The comparison with existing techniques, given in Table 15, for instance, ITS [34], MTS [35], FWA [36], CSA [37], HAS [38], FA [39], SFS [40], SSOE [41], MSSOE [42], CGA-ISP [43], and ARO [44], indicates a stricter justification of the method's efficacy and ensures a fair comparison.

For the IEEE 119-bus test system of Case 2 (determination of DNR alone), hTLBO-CO provided a total loss of 645.09 kW, and a loss reduction of 50.30% relative to the base case. This is considerably higher than all the competitive techniques, whose solutions are typically convergent to levels in the order of 850–867 kW (33–34% loss reduction). Compared to the best solution of the competitor (ARO: 851.01 kW, 34.36%), loss reduction was enhanced by over 15 percentage points. The minimum voltage of 0.9323 p.u. is

comparable to that of the other techniques, albeit slightly lower than ARO's best solution of 0.9412 p.u.

Table 15. Comparison of power loss reduction and minimum voltage for the IEEE 119-bus system (Case 2: DNR only) with state-of-the-art methods.

Method	Opened Switches	Power LOSS (kW)	Loss Reduction (%)	Min Voltage (p.u.)
Initial	118–119–120–121–122–123–124–125–126–127–128–129–130–131–132	1298.09	–	0.8688
ITS [34]	42–26–23–51–122–58–39–95–74–71–97–129–130–109–34	867.40	33.18	0.9323
MTS [35]	42–26–23–51–122–58–39–95–74–71–97–129–130–109–34	867.40	33.18	0.9323
FWA [36]	42–25–23–121–50–58–39–95–71–74–97–129–130–109–34	854.06	34.20	0.9298
CSA [37]	42–25–23–121–50–58–39–95–71–74–97–129–130–109–34	855.04	34.13	0.9298
HSA [38]	23–27–33–43–53–62–72–75–123–125–126–129–130–131–132	854.21	34.19	0.9323
FA [39]	24–26–35–40–43–51–59–72–75–96–98–110–122–130–131	854.06	34.20	0.9323
SFS [40]	23–25–34–39–42–50–58–71–74–95–97–109–121–129–130	854.04	34.20	0.9323
SSOE [41]	23–25–34–39–42–50–58–71–74–95–97–109–121–129–130	853.60	34.16	0.9323
MSSOE [42]	23–26–34–39–42–50–58–71–74–95–97–109–121–129–130	854.03	34.13	0.9323
CGA-ISP [43]	23–25–34–39–42–50–58–71–74–95–97–109–121–129–130	855.04	34.00	0.9290
ARO [44]	23–43–120–51–122–61–39–95–71–74–97–129–130–109–132	851.01	34.36	**0.9412**
Proposed hTLBO-CO	42–25–20–51–47–61–39–125–89–78–90–129–130–108–32	**645.09**	**50.30**	0.9323

Best values in each column are highlighted in bold.

The sequence of switching derived from hTLBO-CO (42–25–20–51–47–61–39–125–89–78–90–129–130–108–32) also deviated significantly from the others, showing the ability of the hybrid approach to discover novel structures of the network different from convergence basins on which the majority of the current schemes become trapped. This diversity of potential solutions and persistent superiority in performance shows the superiority of merging TLBO's exploitation potential with the exploration processes of CO.

In short, the comparison confirms hTLBO-CO's faster convergence, loss reduction, and consistent voltage support, and thereby its ability to outperform existing advanced methods under the same simulated scenario (population size = 50, max iterations = 1000).

5.10. Discussion of Challenges

Although the proposed hTLBO-CO algorithm demonstrates apparent superiority over existing solutions on a range of benchmark systems, there are a couple of challenges to address for its large-scale practical use. Firstly, although the algorithm scaled well to the 119-bus system, its use on extremely large real-world systems containing thousands of buses can require additional approaches, such as decomposition, distributed processing, or GPU acceleration, to further reduce computational overhead. Secondly, although suggested ranges of parameters are provided for the algorithm, sensitivity of the algorithm in unusual operating scenarios—such as extreme loading, extremely tight SOP budgets, or unusual network structures—is yet to be studied. Thirdly, existing simulations also

made deterministic assumptions on load and generation conditions. In practice, the rising integration of renewable energies and uncertainties of the demand side require resilient or stochastic optimization structures capable of incorporating variability explicitly. Moreover, whereas the above study aimed at minimizing loss of power and supporting voltage, further operational considerations—including protection coordination, reliability indices, and dynamic stability—are also necessary to provide for practical realizability of the solutions thus obtained. These challenges also provide avenues for future research and development, wherein the advantages of hTLBO-CO can be combined with uncertainty modeling, high performance computing, and extended system-level constraints to achieve a complete and deployable solution for today's distribution networks.

6. Conclusions

This study has efficiently addressed the computationally complex problem of the simultaneous DNR and SOP integration using a novel hybrid hTLBO-CO algorithm. The proposed algorithm efficiently balances the exploitative power of the TLBO and the exploratory urge of the CO, overcoming the common deficiencies of premature convergence and search stagnation in high-dimensional, mixed-integer nonlinear programming (MINLP) problems. The novelty and performance of hTLBO-CO was rigorously tested on standard IEEE test systems using large-scale simulations. The results clearly show its superiority over a range of current and existing metaheuristics, such as TLBO, CO, PSO, JAYA, and ARO. The impressive capacity of the algorithm is quantitatively verified from a series of valuable results:

- The proposed hTLBO-CO on the IEEE 33-bus network led to a total loss of 74.14 kW for the collaborative DNR-SOP optimization scenario, a 64.44% improvement over the base case and a winning outcome against all opponents.
- For the expanded IEEE 69-bus system, losses reduced further to 40.23 kW for the joint optimization case, an impressive 82.12% improvement.
- Remarkably, on the large-scale 119-bus system—a test case for scalability—the hTLBO-CO performed outstandingly. In the reconfiguration-only scenario, it cut loss by 50.30% (645.09 kW), surpassing the ARO algorithm's best-reported solution of 34.36% reduction by more than 15 percentage points. This result, from a new switching configuration, demonstrates the algorithm's strongest exploration capability in big combinatorial spaces.
- A tight convergence analysis revealed that hTLBO-CO achieved 99% of the ultimate solution much faster and more reliably than competitors, with very minimal final-phase fluctuation (e.g., <0.05% for the 33-bus system), which speaks to its algorithmic efficiency and stability.
- Detailed statistical tests, including Friedman and Wilcoxon signed-rank tests, consistently confirmed the dominance of hTLBO-CO with near-zero p-values ($p < 0.05$), indicating that its performance improvements are statistically significant and not by random chance.
- The Pareto front analysis of the 119-bus system provides system planners with a clear, quantitative trade-off between performance and cost. It identifies strategic zones of compromise, such as the 5-SOP scheme that provided the best voltage profile (0.9573 p.u.) with highly competitive power losses (601.10 kW), providing a data-driven foundation for cost-effective investment planning.

Besides loss minimization, the algorithm also delivered constantly improved voltage profiles, whose minimum voltage levels were always above 0.95 p.u. for Cases 3 and 4, and demonstrated faster and stabler convergence behavior than all comparative methods. Hence, the hTLBO-CO algorithm occupies a place as a scalable, efficient, and extremely

powerful computational tool for the optimal planning and operation of future distribution networks. It provides a solid technology foundation for utilities to employ SOP technology and reconfiguration for increased efficiency and adaptability. Future work will focus on extending the framework to incorporate uncertainties of loads and renewables using stochastic programming, utilizing real-time control of ultra-large-scale grids using high-performance computing, and incorporating constraints of dynamic stability and protection coordination to ensure its practical implementation.

Author Contributions: Conceptualization, A.A. and M.A. (Mohana Alanazi); methodology, A.A.; software, M.A. (Mohana Alanazi); validation, A.A., M.A. (Mohana Alanazi), and M.A. (Mohammed Alruwaili); formal analysis, M.A. (Mohana Alanazi); investigation, M.A. (Mohana Alanazi) and A.A.; resources, A.A.; data curation, M.A. (Mohana Alanazi) and A.A.; writing—original draft preparation, A.A., M.A. (Mohana Alanazi), and M.A. (Mohammed Alruwaili); writing—review and editing, A.A., M.A. (Mohana Alanazi), and M.A. (Mohammed Alruwaili); visualization, A.A., and M.A. (Mohammed Alruwaili); supervision, A.A.; project administration, A.A., and M.A. (Mohammed Alruwaili); funding acquisition, A.A. All authors have read and agreed to the published version of the manuscript.

Funding: The authors extend their appreciation to the Deanship of Scientific Research at Northern Border University, Arar, KSA for funding this research work through project number "NBU-FPEJ-2025-332-01".

Data Availability Statement: The original contributions presented in the study are included in the article; further inquiries can be directed to the corresponding author.

Acknowledgments: The authors gratefully thank Prince Faisal bin Khalid bin Sultan Research Chair in Renewable Energy Studies and Applications (PFCRE) at Northern Border University for their support and assistance.

Conflicts of Interest: The authors declare no conflicts of interest.

References

1. Jayabarathi, T.; Raghunathan, T.; Mithulananthan, N.; Cherukuri, S.H.C.; Sai, G.L. Enhancement of Distribution System Performance with Reconfiguration, Distributed Generation and Capacitor Bank Deployment. *Heliyon* **2024**, *10*, e26343. [CrossRef] [PubMed]
2. Sambaiah, K.S.; Jayabarathi, T. Optimal Reconfiguration of Distribution Network in Presence of D-STATCOM and Photovoltaic Array Using a Metaheuristic Algorithm. *Eur. J. Electr. Eng. Comput. Sci.* **2020**, *4*. [CrossRef]
3. Haggar, M.F.A.; Beshr, E.; Eteiba, M.B. Minimizing Power Loss in Distribution System by Optimal Sizing and Sitting of Distributed Generators with Network Reconfiguration Using Grey Wolf and Particle Swarm Optimizers. In Proceedings of the 2018 IEEE International Conference on Environment and Electrical Engineering and 2018 IEEE Industrial and Commercial Power Systems Europe (EEEIC/I&CPS Europe), Palermo, Italy, 12–15 June 2018; pp. 1–6.
4. Adetunji, K.; Hofsajer, I.; Cheng, L. Trends in the Optimal Location and Sizing of Electrical Units in Smart Grids Using Meta-Heuristic Algorithms. *arXiv* **2019**, arXiv:1910.09312.
5. Jordehi, A.R. DG Allocation and Reconfiguration in Distribution Systems by Metaheuristic Optimisation Algorithms: A Comparative Analysis. In Proceedings of the 2018 IEEE PES Innovative Smart Grid Technologies Conference Europe (ISGT-Europe), Sarajevo, Bosnia and Herzegovina, 21–25 October 2018; pp. 1–6.
6. HassanzadehFard, H.; Jalilian, A. A Novel Objective Function for Optimal DG Allocation in Distribution Systems Using Meta-Heuristic Algorithms. *Int. J. Green Energy* **2016**, *13*, 1615–1625. [CrossRef]
7. Quintero-Duran, M.; Candelo, J.E.; Sousa, V. Recent Trends of the Most Used Metaheuristic Techniques for Distribution Network Reconfiguration. *J. Eng. Sci. Technol. Rev.* **2017**, *10*, 159–173. [CrossRef]
8. Divya, M.; Bindu, R. Ant Colony Optimization Method Applied to Distribution Network Reconfiguration. *Int. J. Adv. Res. Comput. Commun. Eng.* **2013**, *2*, 3817–3824.
9. Kouzou, A.; Mohammedi, R.D. Optimal Reconfiguration of a Radial Power Distribution Network Based on Meta-Heuristic Optimization Algorithms. In Proceedings of the 2015 4th International Conference on Electric Power and Energy Conversion Systems (EPECS), Sharjah, United Arab Emirates, 24–26 November 2015; pp. 1–6.
10. Helmi, A.M.; Carli, R.; Dotoli, M.; Ramadan, H.S. Efficient and Sustainable Reconfiguration of Distribution Networks via Metaheuristic Optimization. *IEEE Trans. Autom. Sci. Eng.* **2021**, *19*, 82–98. [CrossRef]

11. Cikan, M.; Kekezoglu, B. Comparison of Metaheuristic Optimization Techniques Including Equilibrium Optimizer Algorithm in Power Distribution Network Reconfiguration. *Alex. Eng. J.* **2022**, *61*, 991–1031. [CrossRef]
12. Kamel, S.; Hamour, H.; Ahmed, M.H.; Nasrat, L. Atom Search Optimization Algorithm for Optimal Radial Distribution System Reconfiguration. In Proceedings of the 2019 International Conference on Computer, Control, Electrical, and Electronics Engineering (ICCCEEE), Khartoum, Sudan, 21–23 September 2019; pp. 1–5.
13. Tatipally, S.; Ankeshwarapu, S.; Maheswarapu, S. Swarm Intelligence Methods for Optimal Network Reconfiguration of Distribution System. In Proceedings of the 2022 IEEE International Power and Renewable Energy Conference (IPRECON), Kollam, India, 16–18 December 2022; pp. 1–6.
14. Ahanch, M.; Asasi, M.S.; Amiri, M.S. A Grasshopper Optimization Algorithm to Solve Optimal Distribution System Reconfiguration and Distributed Generation Placement Problem. In Proceedings of the 2017 IEEE 4th International Conference on Knowledge-Based Engineering and Innovation (KBEI), Kollam, India, 16–18 December 2017; pp. 659–666.
15. Gomes, Y.R.; Belati, E.A.; Vargas, R. Flower Pollination Algorithm for Distribution System Reconfiguration Problem. In Proceedings of the 2021 IEEE PES Innovative Smart Grid Technologies Conference-Latin America (ISGT Latin America), Lima, Peru, 15–17 September 2021; pp. 1–5.
16. Gomes, Y.R.; Belati, E.A.; Castilla, H.A.P.; Pinto, F.R.; Costa, L.P.M.R. Análise Das Meta-Heurísticas SOS e PSO Aplicadas Ao Problema de Reconfiguração de Rede de Distribuição de Energia Elétrica. In Proceedings of the 2023 15th IEEE International Conference on Industry Applications (INDUSCON), Sao Bernardo do Campo, Brazil, 22–24 November 2023; pp. 997–1004.
17. Mahdavi, M.; Alhelou, H.H.; Bagheri, A.; Djokic, S.Z.; Ramos, R.A.V. A Comprehensive Review of Metaheuristic Methods for the Reconfiguration of Electric Power Distribution Systems and Comparison with a Novel Approach Based on Efficient Genetic Algorithm. *IEEE Access* **2021**, *9*, 122872–122906. [CrossRef]
18. Silva, L.I.; Belati, E.A.; Gerez, C.; Silva Junior, I.C. Reduced Search Space Combined with Particle Swarm Optimization for Distribution System Reconfiguration. *Electr. Eng.* **2021**, *103*, 1127–1139. [CrossRef]
19. Macedo, L.H.; Franco, J.F.; Mahdavi, M.; Romero, R. A Contribution to the Optimization of the Reconfiguration Problem in Radial Distribution Systems. *J. Control Autom. Electr. Syst.* **2018**, *29*, 756–768. [CrossRef]
20. Takano, H.; Murata, J.; Asano, H.; Tuyen, N.D. Reconfiguration of Electric Power Distribution Networks: A Typical Application of Metaheuristics in Electrical Power Field. In *Frontiers in Nature-Inspired Industrial Optimization*; Springer: Singapore, 2021; pp. 111–139.
21. Nassef, A.M.; Abdelkareem, M.A.; Maghrabie, H.M.; Baroutaji, A. Review of Metaheuristic Optimization Algorithms for Power Systems Problems. *Sustainability* **2023**, *15*, 9434. [CrossRef]
22. Adetunji, K.E.; Hofsajer, I.W.; Abu-Mahfouz, A.M.; Cheng, L. A Review of Metaheuristic Techniques for Optimal Integration of Electrical Units in Distribution Networks. *IEEE Access* **2020**, *9*, 5046–5068. [CrossRef]
23. Wang, X.; Wang, C.; Xu, T.; Guo, L.; Li, P.; Yu, L.; Meng, H. Optimal Voltage Regulation for Distribution Networks with Multi-Microgrids. *Appl. Energy* **2018**, *210*, 1027–1036. [CrossRef]
24. Gebru, Y.; Bitew, D.; Aberie, H.; Gizaw, K. Performance Enhancement of Radial Distribution System Using Simultaneous Network Reconfiguration and Switched Capacitor Bank Placement. *Cogent Eng.* **2021**, *8*, 1897929. [CrossRef]
25. Civanlar, S.; Grainger, J.J.; Yin, H.; Lee, S.S.H. Distribution Feeder Reconfiguration for Loss Reduction. *IEEE Trans. Power Deliv.* **2002**, *3*, 1217–1223. [CrossRef]
26. Bhandari, A.S.; Kumar, A.; Ram, M. Grey Wolf Optimizer and Hybrid PSO-GWO for Reliability Optimization and Redundancy Allocation Problem. *Qual. Reliab. Eng. Int.* **2023**, *39*, 905–921. [CrossRef]
27. Rao, R.V.; Savsani, V.J.; Vakharia, D.P. Teaching–Learning-Based Optimization: An Optimization Method for Continuous Non-Linear Large Scale Problems. *Inf. Sci.* **2012**, *183*, 1–15. [CrossRef]
28. Akbari, M.A.; Zare, M.; Azizipanah-Abarghooee, R.; Mirjalili, S.; Deriche, M. The Cheetah Optimizer: A Nature-Inspired Metaheuristic Algorithm for Large-Scale Optimization Problems. *Sci. Rep.* **2022**, *12*, 10953. [CrossRef]
29. Qi, Q.; Wu, J.; Long, C. Multi-Objective Operation Optimization of an Electrical Distribution Network with Soft Open Point. *Appl. Energy* **2017**, *208*, 734–744. [CrossRef]
30. Ji, H.; Wang, C.; Li, P.; Ding, F.; Wu, J. Robust Operation of Soft Open Points in Active Distribution Networks with High Penetration of Photovoltaic Integration. *IEEE Trans. Sustain. Energy* **2018**, *10*, 280–289. [CrossRef]
31. Baran, M.E.; Wu, F.F. Network Reconfiguration in Distribution Systems for Loss Reduction and Load Balancing. *IEEE Trans. Power Deliv.* **1989**, *4*, 1401–1407. [CrossRef]
32. Chiang, H.-D.; Jean-Jumeau, R. Optimal Network Reconfigurations in Distribution Systems. I. A New Formulation and a Solution Methodology. *IEEE Trans. Power Deliv.* **2002**, *5*, 1902–1909. [CrossRef]
33. Zhang, D.; Fu, Z.; Zhang, L. An Improved TS Algorithm for Loss-Minimum Reconfiguration in Large-Scale Distribution Systems. *Electr. Power Syst. Res.* **2007**, *77*, 685–694. [CrossRef]
34. Gupta, N.; Swarnkar, A.; Niazi, K.R. Reconfiguration of Distribution Systems for Real Power Loss Minimization Using Adaptive Particle Swarm Optimization. *Electr. Power Compon. Syst.* **2011**, *39*, 317–330. [CrossRef]

35. Zhu, J.Z. Optimal Reconfiguration of Electrical Distribution Network Using the Refined Genetic Algorithm. *Electr. Power Syst. Res.* **2002**, *62*, 37–42. [CrossRef]
36. Mohamed, E.; Mohamed, A.-A.A.; Mitani, Y. MSA for Optimal Reconfiguration and Capacitor Allocation in Radial/Ring Distribution Networks. *Int. J. Interact. Multimedia Artif. Intell.* **2018**, *5*, 107–122. [CrossRef]
37. Bayat, A.; Bagheri, A.; Noroozian, R. Optimal Siting and Sizing of Distributed Generation Accompanied by Reconfiguration of Distribution Networks for Maximum Loss Reduction by Using a New UVDA-Based Heuristic Method. *Int. J. Electr. Power Energy Syst.* **2016**, *77*, 360–371. [CrossRef]
38. Niknam, T. An Efficient Hybrid Evolutionary Algorithm Based on PSO and ACO for Distribution Feeder Reconfiguration. *Eur. Trans. Electr. Power* **2010**, *20*, 575–590. [CrossRef]
39. Rajaram, R.; Kumar, K.S.; Rajasekar, N. Power System Reconfiguration in a Radial Distribution Network for Reducing Losses and to Improve Voltage Profile Using Modified Plant Growth Simulation Algorithm with Distributed Generation (DG). *Energy Rep.* **2015**, *1*, 116–122. [CrossRef]
40. Tran, T.T.; Truong, K.H.; Vo, D.N. Stochastic Fractal Search Algorithm for Reconfiguration of Distribution Networks with Distributed Generations. *Ain Shams Eng. J.* **2020**, *11*, 389–407. [CrossRef]
41. Zhan, J.; Liu, W.; Chung, C.Y.; Yang, J. Switch Opening and Exchange Method for Stochastic Distribution Network Reconfiguration. *IEEE Trans. Smart Grid* **2020**, *11*, 2995–3007. [CrossRef]
42. Vai, V.; Suk, S.; Lorm, R.; Chhlonh, C.; Eng, S.; Bun, L. Optimal Reconfiguration in Distribution Systems with Distributed Generations Based on Modified Sequential Switch Opening and Exchange. *Appl. Sci.* **2021**, *11*, 2146. [CrossRef]
43. Thanh Nguyen, T.; Nguyen, T.T.; Nguyen, N.A. Optimal Network Reconfiguration to Reduce Power Loss Using an Initial Searching Point for Continuous Genetic Algorithm. *Complexity* **2020**, *2020*, 2420171. [CrossRef]
44. Rao, G.P.C.; Krishna, P.V.R.; Rupesh, M.; Karike, S.; Polisetty, S.; Reddy, S.V.R.; Sreedhar, J. Reconfiguration of the Radial Distribution Network Using an Artificial Rabbits Optimization Approach. *Bull. Electr. Eng. Inform.* **2024**, *13*, 3888–3896. [CrossRef]

Disclaimer/Publisher's Note: The statements, opinions and data contained in all publications are solely those of the individual author(s) and contributor(s) and not of MDPI and/or the editor(s). MDPI and/or the editor(s) disclaim responsibility for any injury to people or property resulting from any ideas, methods, instructions or products referred to in the content.